

Review

# Impacts of Wildfires on Groundwater Recharge: A Comprehensive Analysis of Processes, Methodological Challenges, and Research Opportunities

Mónica Guzmán-Rojo <sup>1,2,\*</sup> , Jeanne Fernandez <sup>3</sup> , Paul d'Abzac <sup>4</sup>  and Marijke Huysmans <sup>2</sup> 

<sup>1</sup> Centro de Investigación Para el Desarrollo Sostenible del Oriente Boliviano, Universidad Católica Boliviana San Pablo, Carretera al Norte Km. 9, Av. Milton Parra., Santa Cruz de la Sierra, Bolivia

<sup>2</sup> Department of Water and Climate, Vrije Universiteit Brussel, Pleinlaan 2, 1050 Brussels, Belgium; marijke.huysmans@vub.be

<sup>3</sup> Department of Earth Sciences, Uppsala University, Villavägen 16, 752 36 Uppsala, Sweden; jeanne.fernandez@geo.uu.se

<sup>4</sup> Centro de Investigación en Ciencias Exactas e Ingenierías, Universidad Católica Boliviana San Pablo, C. Márquez esq. Plaza Trigo, Cochabamba, Bolivia; pdabzac@ucb.edu.bo

\* Correspondence: mguzman@ucb.edu.bo; Tel.: +591-75692088

**Abstract:** Increasing wildfire activity has led to complex ecosystem consequences, with direct effects on the subsystems that affect the presence and movement of water. Although studies have investigated the cascading effects of wildfires on the water balance, our understanding of broad-scale groundwater modifications post fire remains unclear. This review aims to elucidate fire-induced shifts in the water balance, their causal factors, and their potential effects on groundwater recharge. By scrutinizing prior research examples that modeled post-fire recharge scenarios, the review highlights persistent knowledge gaps. The challenge of quantifying and integrating fire-induced alterations in precipitation, wind, and land temperature patterns into recharge projection models is specifically addressed. Despite these gaps, post-fire values of hydrologically meaningful parameters such as leaf area index (*LAI*), curve number (*CN*), and near-surface saturated hydraulic conductivity (*K<sub>ST</sub>*) have been identified. Simulating post-fire recharge via the extrapolation of these values requires the consideration of site-specific conditions, vegetation recovery, and ash removal. It frequently results in a reduced interception and increased surface runoff, while evapotranspiration remains dependent on site-specific factors and often dictates groundwater recharge estimates. Although post-fire recharge simulations are inherently complex and imprecise, their growing application can guide land-use alterations and support policy implementation that considers fire-induced water availability changes.

**Keywords:** groundwater recharge; water-balance processes; wildfire impacts; wildfires; forest hydrology



**Citation:** Guzmán-Rojo, M.; Fernandez, J.; d'Abzac, P.; Huysmans, M. Impacts of Wildfires on Groundwater Recharge: A Comprehensive Analysis of Processes, Methodological Challenges, and Research Opportunities. *Water* **2024**, *16*, 2562. <https://doi.org/10.3390/w16182562>

Academic Editor: Pankaj Kumar

Received: 6 August 2024

Revised: 30 August 2024

Accepted: 8 September 2024

Published: 10 September 2024



**Copyright:** © 2024 by the authors. Licensee MDPI, Basel, Switzerland. This article is an open access article distributed under the terms and conditions of the Creative Commons Attribution (CC BY) license (<https://creativecommons.org/licenses/by/4.0/>).

## 1. Introduction

Most research suggests that wildfire activity has increased in recent decades [1,2] due to a combination of anthropogenic climate change and damaging forest management practices [3–7]. For example, Gillet et al. [8] demonstrated that the rise in burned areas in Canada over the past 40 years can be attributed to human-induced climate change. Flannigan et al. [2] predicted a doubling of burned areas and a 50% rise in fire frequency within certain circumboreal regions by the end of this century. In the past, Siberia, Canada, and Alaska have already been affected by the impact of fire. Similarly, in the Amazon basin, Brando et al. [9] predicted that the burned area by wildfires will double by 2050, impacting around 16% of the region's forests. The escalation of wildfire events is further exacerbated by practices like “chaqueo”, commonly observed in Bolivia, where fires deliberately set for agricultural land clearing often escape control and substantially contribute to the regional fire burden [10,11]. Such trends indicate that in some areas, wildfires will continue to

be a problem exacerbated by human management [12] and could significantly impact water-related ecosystems.

Groundwater discharge from springs and wells is a crucial water supply for numerous communities worldwide [13]. Providing drinking water to almost 50% of the global population [14] directly supports SDG 6 (Clean water and sanitation) by ensuring universal and equitable access to safe and affordable drinking water. It is also the most cost-effective and durable approach to enhance water access for dispersed communities [15–17]. Furthermore, groundwater is less susceptible than surface water to impacts from drought and climate change [18–21]. It can thus provide a hydrological buffer to water availability fluctuations and foster climate resilience in communities [22], aligning with SDG 13 (Climate action) to strengthen resilience and adaptive capacity to climate-related hazards [23,24]. However, as groundwater recharge is a function of rain or snowmelt water interacting with the land cover and its subsequent movement through the subsoil, fire-induced changes in the soil and vegetation can reduce groundwater infiltration and recharge [25]. Groundwater flow systems and water quality parameters evolve dynamically in response to wildfires and climatic stresses [26–28], contributing to uncertainties in groundwater security [26,29]. These post-fire changes threaten water availability, making it more vulnerable to drought and climate-warming effects [30].

The impacts of wildfires on the mechanisms influencing groundwater presence and movement are complex [31]. Direct alterations in a post-fire scenario include surface weathering and the reduction in or damage of vegetation and litter cover [32]. These changes modify the water budget, resulting in altered water distribution among its components, often diminishing groundwater recharge [33,34]. Following a wildfire, the water table may drop, affecting spring discharge and groundwater levels [34]. Conversely, wildfires can also lead to increased recharge rates and enhanced post-fire base flows [35]. Furthermore, fire-induced water partitioning may fluctuate over time, and the decrease in soil moisture can favor subsequent fires by desiccating organic fuel sources [5,36]. Due to the dynamic nature of water distribution after wildfires, projecting water availability is even more challenging.

Growing evidence shows that wildfires trigger cascading impacts water distribution across a variety of spatial and temporal scales [37–41]. Researchers worldwide have studied the effects of wildfires on the water budget through two main approaches. The first approach found that land cover and soil property alterations can modify the magnitudes of water-balance components. These impacts, frequently studied independently, lead to reduced interception and transpiration rates and increased evaporation and runoff rates [6,42–45]. The second approach, at the catchment scale, reveals the occurrence of enhanced peak streamflow and soil erosion rates following a wildfire [42,46–49]. These effects have received more attention than changes in total streamflow due to their more direct measurement and the increased risk posed by sediment loss and transport during peak streamflows [32].

Despite this research, there are several reasons why the impact of wildfires on groundwater recharge remains unclear. First, there is a lack of a comprehensive conceptual framework to support a robust understanding of post-fire groundwater recharge. The interdisciplinary nature of the research, given the numerous impacts triggered by wildfires, has led to a substantial portion of the literature being scattered across technical reports and peer-reviewed academic journals in various disciplines, addressing specific spatial and temporal scales. Second, while post-fire simulation models must be parameterized and validated with independent long-term data [50], the evolution of the post-fire hydrological response over time causes the parameters to fluctuate. Hydrological processes that depend on the regenerative capacity of vegetation and the washing of ashes from the soil could be more dynamic. Unfortunately, validation is typically not possible since pre- and post-fire hydrologic and hydrogeologic measurements are often unavailable [51]. In practice, obtaining baseline groundwater levels in fire-prone areas proves challenging due to the unpredictable nature of wildfires and the high cost of long-term groundwater monitoring [51]. This highlights the need for further research to establish a comprehen-

sive conceptual framework and enhance our understanding of the impact of wildfires on groundwater recharge.

Moreover, studies on the long-term impact of fires on groundwater recharge have produced conflicting results. Some have suggested that the reduction in soil moisture and infiltration following a fire can lead to a decrease in groundwater recharge [52–54]. Conversely, others have indicated that reduced water loss through precipitation interception can increase soil moisture and groundwater recharge [37,55,56]. Some studies supporting these findings are based on direct observations [48,57–59]. Moreover, Atchley et al. [51] demonstrated that the severity of wildfires can be a determining factor that can either increase or decrease groundwater recharge. For example, high-severity wildfires can drastically reduce soil permeability, resulting in a significant increase in runoff as the dominant process. Consequently, the increased runoff reduces the amount of water available for infiltration, thereby decreasing groundwater recharge.

This review comprehensively explores the impacts of wildfires on the water balance and groundwater recharge by examining each water-balance component and providing guidance for their incorporation into medium- and long-term catchment-scale simulations. Initially, the soil–water balance is elucidated, focusing on its primary components and the effects wildfires may have on them. Qualitative information is provided, and the variables most sensitive to these changes are highlighted. Subsequently, how past studies have estimated these variables and parameters on small scales immediately following a fire is reviewed, illustrating their temporal evolution using examples of integration into water-balance simulations. The feasibility of incorporating these changes into post-fire recharge simulations is also examined. This process also considers site conditions and temporal scales. Finally, gaps and research opportunities are identified to enhance recharge estimation at larger scales. By addressing these gaps, we aim to improve the estimation of recharge on a larger scale, ultimately informing decision-making processes related to land-use changes in fire-prone regions that rely heavily on groundwater resources.

## 2. Examining the Influence of Wildfires on Water Budget and Groundwater Recharge

Assessing groundwater recharge has progressed from a scientific interest to a pressing and crucial matter in hydrogeological research. Quantifying groundwater recharge rates is essential for effective and sustainable groundwater management, as groundwater is critical in preserving ecosystem services [60–63]. Nevertheless, its spatial dynamics in a forest result from a series of complex interacting processes [64], making recharge estimation challenging. Numerous methods exist for estimating groundwater recharge, most of them based on the physical principle of water budget [65]. Employing this approach, the processes can be reduced to a system of water storage components and water movement as solid, liquid, or gas within and between these components [37]. As a result, recharge can be estimated as the residual of this balance, namely the difference between the volume of precipitation and the portion that fails to infiltrate.

In forests, the partitioning of rainfall into interception, evapotranspiration, runoff, and soil water recharge is intimately linked to the presence of vegetation [64,66,67]. As described by Jost [64], typically, lower runoff rates and higher evapotranspiration rates are simulated in forests compared to other land covers [68–70]. Evapotranspiration, for instance, is particularly sensitive to variations in the physiological characteristics of vegetation, leading to significant fluctuations if vegetation is altered or removed [64,71]. Consequently, events that substantially modify land cover will result in changes to water distribution [72]. Alterations to land cover cause changes in water distribution patterns and related properties, including hydraulic ones [73]. These changes are crucial for preserving ecosystem resilience and managing water resources effectively in the face of environmental disturbances [72].

Wildfires directly affect land cover by burning vegetation and litter as well as depositing ash on the land surface. As illustrated schematically in Figure 1, these alterations influence all hydrological processes, including groundwater recharge [74]. The cascading effects on water balance can be divided into three phases. First, following a wildfire,

the diminished canopy leads to reduced interception, resulting in a higher water surplus (runoff + groundwater recharge) [35]. Second, the increased volume of water reaching the soil surface compacts or dislodges it due to raindrop splash [75]; this effect, combined with ash deposition, increases runoff and alters soil properties [76]. Third, the absence of shade and changes in surface albedo [77] are thought to increase evaporation after wildfires [36]. These divergent redistributions of water following wildfires underscore the importance of understanding the effects of such events on water budget and the need for their joint quantification for recharge estimations purposes [78].

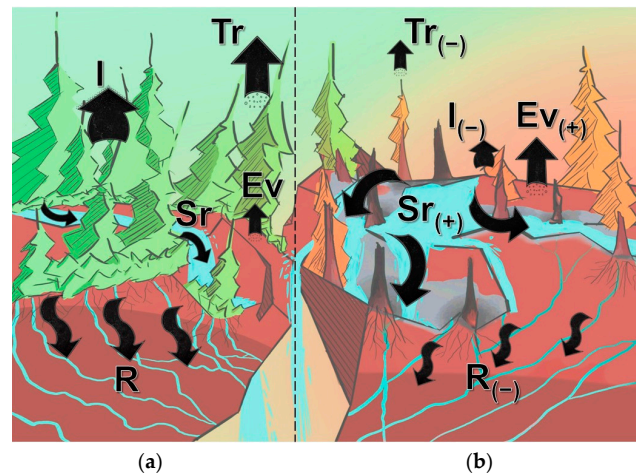


**Figure 1.** Schematic representation of hydrological processes in a forest ecosystem, illustrating the hypothesis that altered water-balance components contribute to reduced groundwater recharge after a wildfire. Subfigure (a) shows the region before the wildfire, highlighting normal hydrological processes. Subfigure (b) focuses on the same region after being heavily affected by high-intensity wildfires, detailing the cascading effects on water cycle components: interception (I), transpiration (Tr), evaporation (Ev), surface runoff (Sr), and recharge (R).

Meteorological variables, including precipitation, temperature, and wind velocity, play a crucial role in shaping the microclimate that influences water balance within a specific area [79]. These variables can be affected after a forest fire, subsequently impacting water recharge [80]. Additionally, the canopy loss eliminates the buffering effect and enhances wind flux, which, along with changes in albedo, promotes evaporation. However, as fire does not directly modify these variables, correlations are complex and dependent on various factors, such as regional climatic patterns [79]. Furthermore, the spatial heterogeneity of a wildfire's impact and the forest's varying recovery capacity results in a higher difficulty level. The complexity and interdependence of these mechanisms and their implications for water management highlight the need for increased efforts to understand and conceptualize them [80].

### 3. Soil-Water-Balance Components and Their Post-Fire Response: An Overview

#### 3.1. Exploring the Complexity of Post-Fire Precipitation and Its Implications for Water-Balance Management

Rainfall plays the most significant role in a watershed, as it controls the amount of available water. In a post-fire situation, changes in surface properties can indirectly impact rainfall [74]. Fire-induced removal of vegetation and the reduction of surface albedo alter humidity and surface temperature, which in turn affect precipitation through feedback mechanisms [81]. For example, the post-fire albedo influences the rate at which soil dries in burned areas compared to unburned areas. These new conditions increase the occurrence of convective storms [82]. The literature has shown that post-fire floods are more frequent and are sensitive to precipitation following wildfires [74,83]. However, this does not necessarily reflect changes in precipitation metrics themselves. Instead, peak flows tend to increase due



to a combination of increased rainfall and reduced soil permeability [84]. Consequently, understanding post-fire rainfall is necessary both independently and on larger time scales to better manage water resources in the face of increasing wildfire risks [74,84,85].

In continuous water-balance models, rainfall is typically expressed as cumulative depth over a given interval [81]. Some models also incorporate storm-related metrics indirectly within their empirical dependencies. For example, the number of rainy days is a metric used by specific models to estimate the water interception threshold [86]. This then affects the interception calculation, which is calculated on a monthly basis. Although post-fire precipitation amounts can be easily measured with a rain gauge, the challenge lies in determining which precipitation metrics best reflect post-fire responses [81]. Moody et al. [81] outlined a variety of precipitation metrics, categorizing them into four groups. These range from typical time-dependent metrics such as total rainfall to qualitative metrics related to the origin of the rainfall, such as convective rain. The latter is associated with rainfall redistribution on a smaller scale. Additionally, it is crucial to determine how to incorporate these metrics into post-fire interception calculations and subsequent water distribution estimations. However, the potential for upscaling to larger areas warrants further discussion. Incorporating fire-induced rain into post-fire conceptual models may be possible if long-term post-fire trends for this metric are identified, allowing analysts to make consistent projections.

### *3.2. Fire-Induced Albedo Alterations and Evapotranspiration: Analyzing Recovery Patterns and Vegetation Response*

Interception and evapotranspiration are crucial water-balance components significantly affected by fires. Vegetation plays an essential role in interception and transpiration, leading to a cascade of impacts on other hydrological processes [87]. As previously mentioned, reducing leaf cover and, therefore, interception results in increased water availability for infiltration and runoff. Neary et al. [37] described how both vegetative canopies and accumulations of litter and decomposed organic material on the soil surface can disrupt the penetration of rainfall into the soil layer. High-severity wildfires diminish interception, thereby decreasing the amount of water available for evaporation. In mature forests, a substantial portion of precipitation intercepted by leaves evaporates [37]. Moreover, leaf combustion considerably reduces transpiration [35] since vegetation primarily transpires through leaves. Vegetation recovery after a fire is important for restoring the ecosystem's hydrological functions, though it is not always guaranteed. These observations underscore the intricate relationship between wildfires and water distribution mechanisms, whose joint action must be framed in the water budget.

Veraverbeke et al. [88] described that charring-induced ground surface blackening after a fire reduces surface reflectance or albedo [89–93]. Lower albedo increases net surface radiation, the primary energy source for the evaporation process [94], thereby enhancing evapotranspiration rates post wildfire. However, this impact is brief, as albedo rapidly returns to its pre-fire levels once burnt materials are cleared away by weather and once the ground vegetation regenerates [93]. In fact, some studies reveal that albedo may exceed pre-fire values in the medium term [88,90]. As described by Veraverbeke [88], albedo values are highly sensitive to surface conditions, and fire-induced changes in albedo can range from one year in grasslands [89] to several decades in forests [91]. This highlights the differences between forest types and their stationarity. The regeneration of ground vegetation not only restores ecological functions but also modifies the albedo, which is critical for regulating future evaporation rates [95]. Consequently, conceptually modeling these post-fire mechanisms necessitates detailed knowledge of the vegetation and its projected changes, as it is influenced by land use and vegetation recovery capabilities.

### *3.3. Impacts of Fire on Soil Infiltrability and Runoff Generation*

Runoff and recharge are closely interrelated mechanisms that are also affected by fire. Research has revealed considerable variability of pre- and post-fire runoff dynamics due to

wildfire effects across various environments. Changes in land cover and fire dynamics can alter soil infiltrability [96], leading to increased runoff and potentially decreased infiltration. Removing the highly porous and organic-rich upper soil layers results in pore sealing due to rain splash and ash particulates [97–99], while ash removal through natural processes like rainfall and wind can facilitate soil recovery [100]. As vegetation regenerates, it stabilizes the soil and mitigates this hydrophobic effect, thus improving soil infiltrability and reducing runoff [101]. Conversely, soil heating alters both physical and chemical properties, affecting water-repellency behavior and aggregate stability. [102–104]. The soil aggregates suffer a reduction in size with the fire and become less stable [87]. These alterations lead to higher surface overland flow, particularly peak flows [32], which have been the focus of numerous studies in the past two decades.

The soil surface dynamics during and after a wildfire lead to decreased soil infiltrability [42,105,106] in the topmost centimeters, thereby increasing surface water flow (Figure 2). Moody et al. [42] suggested three possible reasons for this: the removal of highly porous and organic layers that created obstructions, increasing frictional drag during runoff; pore compaction and sealing by splashing raindrops, exacerbated by the removal of plant cover; and the soil water repellency effect produced as a consequence of alterations in the soil's physical and chemical properties caused by heating. In practice, runoff can be estimated using runoff coefficients, which are typically higher in post-fire conditions, leading to increased surface overland flow and enhanced peak flows [32]. The heightened risk of flooding has prompted the investigation of the connection between runoff response and wildfires using episodic rainfall-runoff models, with hydrological parameters such as runoff coefficients serving to quantify this relationship. To ensure accurate hydrological modeling, these coefficients require adjustments reflecting both the type of ash deposits and any vegetation recovery, as these factors significantly influence soil infiltrability and runoff dynamics [100,107].

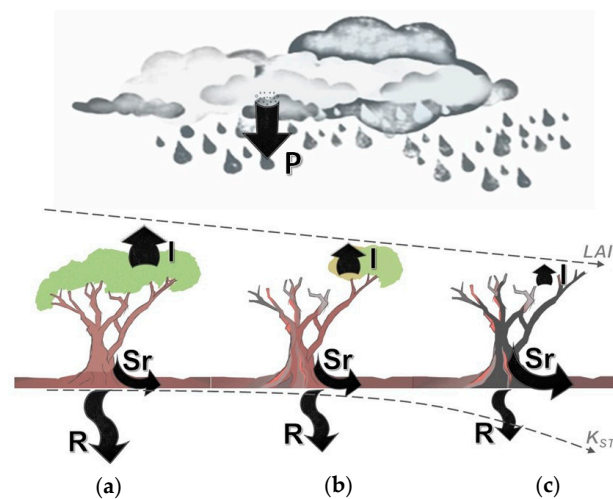


**Figure 2.** Representation of the interaction between interception ( $I$ ) and runoff ( $S_r$ ) based on the description by Atchley et al. [51], depicting (a) natural conditions, (b) moderate-intensity fires, and (c) high-intensity fires. The linear decrease in Leaf Area Index ( $LAI$ ) and the exponential decrease of saturated hydraulic conductivity ( $K_{ST}$ ) characterized by Moody et al. [108] are illustrated.

Fire-induced changes in soil properties have gained significant attention over the past two decades [32] due to their critical impact on infiltration excess and the recharge process [109]. These changes in parameters related to various infiltration equations have been characterized [109]. The saturated hydraulic conductivity ( $K_{ST}$ ) has been extensively studied and is known to experience long-term changes due to fire. Like most other metrics, fire's effects on  $K_{ST}$  are typically confined to patches of ashes [81] and are more significant in the top 1 cm of soil [75]. Fire-induced water-repellent effects are typically restricted to areas beneath canopies [105] and act synergistically to reduce infiltration while increasing

the generation of surface runoff [110]. A key finding is that reductions in  $K_{ST}$  are often associated with the collapse of the most prominent near-surface pores due to the loss of soil stability caused by heating [32,109]. This promotes the persistence of lower  $K_{ST}$  values over time, prolonging increased runoff. Consequently, relationships have been established that link  $K_{ST}$  fire-induced alterations with the differenced normalized burn ratio ( $\Delta NBR$ ) [111]. Simple ratios have also been proposed to parameterize infiltration models on a larger scale [109]. A critical focus of current research is the development of improved techniques for numerically simulating infiltration in burned areas, considering soil and ash properties [110].

#### 4. The Feasibility of Incorporating Changes in Post-Fire Recharge Simulations: Lessons Learned from Past Studies

As mentioned, estimating recharge within the water budget framework relies on accurately determining other water budget components. Different methods can be used to estimate each component, and the integration is usually performed through numerical continuum models. These models apply the mass balance equation at the model-cell level, considering non-uniformity at larger scales. [65]. The processes in each cell are set in a cascading way such that there is an order of occurrence of the processes affecting water [112]. After the precipitation event, rain interception by the forest canopy, runoff/infiltration, evapotranspiration, and ultimately groundwater recharge are affected. In practice, implementing this approach has been limited due to scarce information, resulting in empirical dependencies in the processes involved in these models. Most of them comprise parameters obtained from detailed soil and land-use maps. Consequently, the accuracy of current practices for recharge estimation depends on the accuracy of the water-balance components and hence the quality of the inputs.

Upon validation, water-balance models can simulate future groundwater recharge scenarios under varying regional conditions, adjusting to represent the impacts of surface changes on recharge rates [113]. Analysts require hydrological inputs reflecting post-fire conditions to employ this approach for post-fire scenarios [114]. Experimental studies comparing pre- and post-fire vegetation type/species, soil, and climate conditions provide valuable inputs. While this was once a constraint, the growing availability of published values, ranging from ratios to nonlinear functions linking pre- and post-fire metrics, enables estimating recharge rates for various post-fire scenarios. Nonetheless, these alterations should be cautiously extrapolated to different site conditions.

##### 4.1. Fire Severity and Post-Fire Metrics

Numerous methods exist for quantifying the impact of wildfires based on the principle that measurable contrasts between burned and unburned environments are present in space and time [115]. Despite recent studies highlighting terminology issues [116–118], two definitions and various metrics commonly appear in the literature to address these contrasts. Both are related to severity, often loosely defined as “the magnitude of ecological change due to the fire” [116–118]. Fire severity, based on the first definition, infers vegetation and soil changes occurring within minutes to hours [117,119]. The second definition of burn severity typically describes the long-term effects of fire, ranging from weeks to decades [116,120]. This latter definition encompasses accumulated changes in ecological communities that compose the landscape and is framed by our interpretation [111] and hence can have a considerable impact on the long-term environmental and hydrological processes [121].

Assessing the severity of burn is commonly done at the landscape level by utilizing remote sensing mapping techniques [117]. The difference between pre-fire and post-fire conditions provides the basis for mapping large fires on public lands [77,122–124]. The most frequently used technique for determining burn severity is the normalized burn ratio ( $NBR$ ) [117]. Key and Benson [111] described how this metric integrates two Landsat bands (4 and 7) that respond most to burning but in opposite ways [111]. Band 4 measures

the reflected radiation from vegetation in the near-infrared range ( $0.76\text{--}0.90 \times 10^{-6}$  m). After a fire, vegetation typically decreases, resulting in a decrease in the reflected radiation measured by band 4. On the other hand, band 7 measures the reflected radiation from bare soil in the short-wave infrared range ( $2.08\text{--}2.35 \times 10^{-6}$  m), which typically increases following a fire. [42]. The *NBR* is calculated as shown in Equation (1), where *R* values represent satellite reflectance quantities per band computed per pixel after atmospheric transmittance correction. The resulting change in normalized burn ratio ( $\Delta NBR$ ), calculated using Equation (2), distinguishes burned from unburned areas, providing a quantitative measure of the change. Given the critical role of *NBR* in distinguishing burned from unburned areas, this metric proves indispensable for refining hydrological modeling and ecological assessments, directly linking the satellite-derived measurements to practical applications in managing post-fire landscapes.

$$NBR = \frac{R4 - R7}{R4 + R7} \quad (1)$$

$$\Delta NBR = \frac{NBR_{pre\ fire}}{NBR_{post\ fire}} \quad (2)$$

Burn severity is typically classified into discrete descriptive classes, such as high (>640), moderate (315 to 640), and low (70 to 315) [125,126]. According to Moody et al. [42], these classes aim to reflect the degree of canopy layer removal, which intercepts rain, and the removal of ground cover, litter, and duff (decayed organic matter) layers. For example, Benavidez-Solorio and MacDonald [127] found that after a high-severity fire, the surface organic layer is entirely consumed, and the surface layer of the underlying mineral soil is altered. In contrast, after low-severity fires, only a portion of litter and duff are burnt, as there is less soil exposure to fire. These changes in post-fire land cover have distinct effects on water redistribution. As a result, certain fire impacts on a region's hydrology have been associated with the burn severity [37,128], as exemplified in the following sections.

#### 4.2. Long-Term Interception and Evapotranspiration Estimates Focused on Continuous Water-Balance Models

Evapotranspiration and interception are both functions of vegetation density, specifically canopy foliage content [51]. This characteristic is often measured, analyzed, and modeled across various spatial scales as leaf area index (*LAI*) [129]. *LAI* refers to the leaf area ( $\text{m}^2$ ) within a canopy per unit ground area ( $\text{m}^2$ ) and is broadly considered as a basic descriptor of vegetation condition across various studies. [129]. Reduced post-fire *LAI*, in addition to decreasing interception, alters evapotranspiration rates. If soil water is not limited, transpiration will be constrained by leaf area [130,131]. Some studies have examined fire-induced *LAI* alterations and linked *LAI* to burn severity [51,132]. For mixed conifer vegetation, Atchley et al. [51] estimated post-fire *LAI* values using allometric functions for  $\Delta NBR$ . Simulations were conducted using the continuous water-balance model ParFlow-CLM (Version 895) [133,134] with the conclusion that the ascribed alteration in *LAI* drives the simulated response of decreased evapotranspiration through transpiration reduction. This shows that transpiration reduction is closely related to vegetation density, which is proportional to *LAI* [72,135].

Increased evaporation is associated with reduced aerodynamic resistance, as it becomes easier for the wind to mobilize water vapor [136]. The Penman-Monteith method, which incorporates this variable in intermediate computations, is widely recognized by the scientific community for its accuracy in estimating evapotranspiration rates under diverse global conditions [137,138]. This method's high precision can be attributed to its consideration of energy and aerodynamic factors [139].

In the context of forest fires, the Penman-Monteith method's usefulness may not change significantly, as the equation accounts for altered aerodynamic resistance, radiation balance, and vapor pressure deficit. However, changes in vegetation characteristics such as leaf area index (*LAI*) and canopy structure may impact the method's accuracy by altering



parameters like aerodynamic resistance and surface albedo [67]. Thus, it is crucial to consider these vegetation changes when applying the Penman-Monteith equation to post-fire scenarios. Also, time scales must be considered, as new land use or forest regenerative capacity change parameters. Consequently, simulating post-fire scenarios by utilizing fire-induced *LAI* is possible if there is an understanding of vegetation cover depletion and regeneration processes [140].

As previously mentioned, fire disturbances have been found to reduce surface albedo [51], which is a sensitive variable used for estimating actual evapotranspiration by calculating net radiation through the balance between incoming and reflected solar radiation [88,137]. Albedo is incorporated in evapotranspiration estimation methods ranging from the standardized Penman-Monteith approach to remote sensing-based techniques grounded in the energy balance equation [44]. However, albedo's complex temporal dynamics and high sensitivity make post-fire albedo inference challenging. Veraverbeke et al. [88] studied the effects of the 2007 Peloponnese wildfires in Greece on broadband surface albedo changes using MODIS satellite imagery. They observed a strong initial drop in albedo, followed by diminishing fire-induced changes as seasonality began to dominate the time series.

Post-fire albedo dynamics, including a sharp decrease immediately after the fire event and varying increases during summer and winter periods, complicate correlations with fire severities in the literature [88–90,92,93]. This makes incorporating post-fire albedo into long-term evapotranspiration estimates complex and uncertain due to time scale and vegetation type considerations. Areas with high-severity burns exhibit significantly higher post-fire albedo during spring and faster increases during summer than moderate and low-severity burns [141]. Moreover, deciduous ecosystems have higher summer albedo than evergreen forests, while winter differences are more minor [88]. Although albedo is sensitive, its tendency to recover pre-fire values over time suggests that modifying this variable in long-term evapotranspiration rate estimation and water-balance models may be irrelevant.

#### 4.3. Post-Fire Runoff and Infiltration Dynamics: Approaches from Peak Flow Model Studies

Over the past two decades, peak flows have been the subject of numerous studies. Runoff has been extensively studied in catchments [142], and its estimation typically depends on runoff coefficients. These empirical and widely used parameters represent how easily non-infiltrated water can move over the land surface for a given rainfall and may have variants depending on the methodology used. Curve number (CN) analysis is one of the most well-known approaches developed by the Soil Conservation Service (SCS) in the United States (now the Natural Resources Conservation Service; NRCS) [143,144]. The SCS-CN method has been widely used to predict runoff from watersheds due to its straightforward conceptual basis [53]. In this method, the runoff is determined using the CN, which reflects the combined effects of soil type, land cover, and antecedent soil moisture conditions on runoff generation [145].

The CN and other coefficients involved in the runoff process are also used in continuous models, but they are not the same as those employed in episodic models. The reason is that these coefficients and their correction factors are developed for specific methods that are not always comparable. Furthermore, their operation within episodic models differs from continuous models. The runoff process contains thresholds of rainfall intensity and duration [109], which differ significantly from monthly accumulation to storm events. However, the Soil Conservation Service curve number (SCS-CN) has also been employed in numerous continuous simulation models since the 1980s [146]. For example, Rodriguez et al. [33] applied an adjusted curve number (CN) through the SWAT model to anticipate the impacts of fire on infiltration and runoff. In Batelis and Nalbantis' study [52], a modified CN was applied under the premise that less permeable patches of ashes are formed under the burned vegetation, resulting in a quadratic decrease in infiltration rates for different percentages of burned area. Given these differences, refining the curve number is crucial in post-fire scenarios through experiments that monitor streamflow in burned watersheds. Adjustments should account for the variability in vegetation types and the unique charac-

teristics of ash, which collectively have a profound impact on soil permeability and runoff dynamics, enhancing the precision of hydrological models.

In the literature, continuous models based on mass balance often integrate runoff coefficients in their estimates. Since runoff is frequently one of the final outputs of these models, its computation is affected by intermediate results from previous processes directly influenced by the fire. Moreover, the recalculation of runoff coefficients for every time step can be conducted as a function of antecedent humidity [33] or using more empirical and simplified approaches, such as correcting the runoff coefficient based on fire-induced evapotranspiration. Consequently, changes in runoff involving a runoff coefficient (or equivalent) must be carefully incorporated along with parameters reflecting post-fire conditions in other water-balance components. Adjustments to runoff coefficients are essential to accurately model hydrological responses in burned areas, taking into account changes in vegetation and ash properties that significantly influence the water balance.

Water-balance models are often coupled with groundwater flow models in an interactive process to enhance the accuracy of model outputs. This approach is adopted because fluctuations in the water table can impact other balance components, which, in turn, affect the water table. Groundwater depth recalculations specifically influence evapotranspiration and runoff components. A decrease in groundwater levels can induce lower rates of evapotranspiration and reduced soil humidity, thereby buffering runoff rates. In models like WetSpass, for instance, a runoff correction factor ( $C_h$ ) can be set as a function of evapotranspiration. Similarly, subsurface flow models can be coupled with water-balance models, requiring consideration of spatial variability through the concept of patches or, more precisely, a patch mosaic with variable thickness [81].

Atchley et al. [51] incorporated lower permeability layers through this type of assembly, demonstrating that reduced infiltration plays a predominant role in the distribution between infiltration and runoff for high-fire severities. Atchley also showed that post-fire evapotranspiration reduction is a more dominant process than water loss through terrestrial flow in continuous models. However, in cases of high fire severity, surface flow can dominate the water balance, leading to a turning point that results in drier conditions.

Fire-induced parameter changes linked to different infiltration equations have been characterized [109]. Saturated hydraulic conductivity ( $K_{ST}$ ) is one of the most studied properties because of its importance in the infiltration process. Fire effects on  $K_{ST}$  are usually confined to ash patches [81] and are more pronounced in the top 1 cm of soil [75]. Water-repellent effects from fire are typically limited to areas beneath canopies [105], reducing infiltration and amplifying surface runoff generation.

One of the more critical findings is that reductions in  $K_{ST}$  are typically associated with the collapse of the largest near-surface pores due to the loss of soil stability from heating [32,109]. This promotes the persistence of lower  $K_{ST}$  over time, prolonging the increased runoff. Relationships connecting  $K_{ST}$  fire-induced alteration with  $\Delta NBR$  have been established [111]. Simple ratios have been proposed to parameterize infiltration models on a larger scale [109]. Recent studies are focused on improving methods for numerically modeling infiltration in areas affected by fires, considering soil and ash and incorporating these changes into physically based models [110]. This will require improved parameterization of hydraulic conductivity through site-specific infiltration tests after a fire, accounting for the dynamic post-fire soil evolution.

Tables 1 and 2 present examples of relationships that can aid in model parameterization for post-fire simulations. Some parameters, such as post-burn runoff, appear more sensitive to soil type, as demonstrated by values for ash patches proposed by Batellis and Nalbantis [52] using a modified version of the SCS-CN method for different soil types. Other parameters, like unsaturated hydraulic conductivity, vary exponentially and depend more on burn severity than soil type.

**Table 1.** Summary of the most significant hydrological parameters/variables that change after a fire and their importance in the context of estimating recharge.

| Component   | Approximate Relationship with $\Delta NBR$  | Initial Change in the Component Relative to Unburned Value   | Post-Fire Timeline  | Context and Study Reference   | Relevance to Long-Term Groundwater Recharge  |
|---|---|--|---|---|--|
| Leaf Area Index (LAI)                               | Linear ( $\downarrow$ )   | Decreases by approximately 34.0% (low severity) to 96.5% (high severity). Recovery to 90–108% of pre-fire levels during regeneration.  | <p>The diagram shows a horizontal bar representing LAI. The left portion is labeled 'Pre-fire values' and is dark grey. A vertical line marks the fire event. To the right, the bar drops significantly, labeled 'Post-fire values'. An arrow points to the right from the fire event, labeled '(+) regeneration', indicating the start of recovery. The bar gradually rises back towards the pre-fire level over time.</p>   | Estimated for a mixed conifer vegetation community in New Mexico [51] and for deciduous grasses and shrubs in Canada [141].       | Moderate, indirect impact; applicable only when regeneration is absent since severe crown damage could negatively affect the survival of burned trees [140]. |
| Albedo ( $\lambda$ )                                | Linear ( $\uparrow$ ) after the first year  | High-severity wildfires cause a 52% spring albedo increase, rising to 76% after 5–7 years, significantly larger than the 16% summer albedo decrease (26% later). The severity gap reaches 60%.                       | <p>The diagram shows three horizontal bars representing different albedo components. The top bar is labeled 'Spring albedo' and shows a sharp increase from a dark grey pre-fire level to a lighter grey post-fire level. The middle bar is labeled 'Summer albedo' and shows a decrease from a dark grey pre-fire level to a lighter grey post-fire level. The bottom bar is labeled 'Severity gap' and shows a dark grey bar that remains constant over time. Vertical dashed lines indicate time intervals: hours, days, months, years, and decades.</p> | Estimated for 4 Canadian ecozones dominated by needleleaf forests, broadleaf/mixed forests, and closed and open shrublands [141]. | Low, indirect impact; it does revert to its original value; however, special attention should be paid to the spring albedo.                                  |
| Curve number for normal moisture conditions (CN II) | Inferred through burn patch formation ( $\uparrow$ ) associated with soil-based characteristics | Ash patch values range from 77 (sand) to 94 (clay), representing an increase between 71% and 13% of their pre-fire values in a broad-leaved forest. These values persist for at least the following 1.5 years [128]. | <p>The diagram shows a horizontal bar representing the curve number. It shows a sharp increase from a dark grey pre-fire level to a lighter grey post-fire level. The bar remains at this higher level over time. Vertical dashed lines indicate time intervals: hours, days, months, years, and decades.</p>   | Distinct ash patch values suggested by Batellis and Nalbantis [52] for various soil types (A, B, C, and D).                       | High; it does not revert to its original value and is directly linked to recharge.   |
| Saturated hydraulic conductivity ( $K_{ST}$ )       | Exponential decrease ( $\downarrow$ ) for low severity wildfires; no changes observed           | Variability ranges up to 93% in soil with 4 cm pre-fire litter-duff depth consumed after a high-severity fire.   | <p>The diagram shows a horizontal bar representing saturated hydraulic conductivity. It shows a sharp decrease from a dark grey pre-fire level to a lighter grey post-fire level. The bar remains at this lower level over time. Vertical dashed lines indicate time intervals: hours, days, months, years, and decades.</p>  | Adjusted for sandy loams ( $K_{ST} = 0.0325$ m/h) based on Atchley et al. [51], in reference to Moody et al. [108].               | High; it does not revert to its original value and is directly linked to recharge.   |

**Table 2.** Summary of some relations that link hydrological parameters with alterations caused by three regimes of wildfires.

| Component \ Wildfire Severity Scenario $\Delta NBR$             | 70 < Low < 315  | 315 < Moderate < 640  | 640 < High   | Guidelines for Its Application and References  |
|---|---|---|--|--|
| <i>P</i>  |   |   |  |  |
| <i>I</i>  |   |   |  |  |
| ↓ Leaf Area Index ( <i>LAI</i> )                                | $LAI = (0.696 \pm 0.095) \times$<br>unburned value              | $LAI = (0.66 \pm 0.03) \times$ unburned value   | $LAI = (0.035 \pm 0.005) \times$<br>unburned value | Estimated for mixed conifer vegetation community [51].   |
| ↓   | Daily interception threshold $I_D = F(LAI)$                     |   |  | Equation introduced by De Groen and Savenije [147] to estimate the average monthly interception.   |
| <i>Sr</i>   |   |   |  |  |
| ↑↑ Curve number for normal moisture conditions ( <i>CN II</i> ) | $CN II = 77 (A), 86 (B), 91 (C), 94 (D)$                        |   |  | Unique values for ash patches proposed by Batellis and Nalbantis [52] for different types of soil (A, B, C, and D) through a modified version of the SCS-CN method on a daily basis.   |
| ↓↓ Saturated hydraulic conductivity ( $K_{ST}$ )                | $K_{ST} = \text{constant} =$ unburned value                     | $K_{ST} = 2360 \times \exp(-0.0056 \times \Delta NBR)^a$<br>$K_{ST} = 390 \times \exp(-0.0056 \times \Delta NBR)^b$ |  | <sup>a</sup> Estimated for sandy loams ( $K_{ST} = 0.147$ m/h) for $420 < \Delta NBR < 886$ [108]. <sup>b</sup> Adjusted for less permeable sandy loams ( $K_{ST} = 0.0325$ m/h) [51]. |
| <i>ET</i>   |   |   |  |  |
| ↓ Albedo ( $\lambda$ )  | $\lambda = (0.13 \pm 0.06) +$<br>unburned value                 | $\lambda = (0.16 \pm 0.06) +$ unburned value  | $\lambda = (0.20 \pm 0.06) +$<br>unburned value    | For spring albedo in four Canadian ecozones with needleleaf forest, broadleaf/mixed forest, and closed and open shrublands [141].  |
| ↑   | Surface resistance $r_s = F(LAI)$                               |   |  | Estimation used by most methods [148].   |
| ↓   | Crop coefficient $K_{CFAO} = F(LAI)$                            |   |  | Crop coefficient for natural vegetation proposed by Monteith [149].  |
| <i>R</i>  |   |   |  |  |
| Water-balance equation ( <i>R</i> )                             | $R = P - I(\downarrow) - ET(\uparrow\downarrow) - Sr(\uparrow)$ |   |  |  |

*LAI* exhibits a strong linear dependency with burning, affecting interception [51] and additionally impacting post-fire evapotranspiration. These post-fire values, derived from specific sites, provide practical examples of how disturbances have been incorporated into specific water budget components. The linear relationships reported in the literature represent a small fraction of the available knowledge; continued literature review may uncover new insights applicable to specific study sites. Future research should focus on deriving these relationships for a more diverse range of environments.

Wildfires have been shown to influence all water-balance components, including recharge. Fire-induced alterations can lead to reduced interception and increased runoff, resulting in less evident impacts on recharge. These processes tend to counteract each other due to the magnitudes of highly sensitive parameters involved in both mechanisms. Furthermore, wildfire-driven changes influence various aspects of the water balance, such as evapotranspiration, soil moisture, and groundwater levels, ultimately affecting the overall water balance in a given region [74,97,109]. Consequently, it is crucial to analyze these interactions within site-specific conditions.

## 5. Modeling the Impacts of Wildfires on Groundwater Recharge: Challenges and Opportunities

Although parameters such as *LAI* have been studied, and some post-fire data are available, it is crucial to continue characterizing them due to their direct impact on interception. In the case of runoff, the rapid increment of this process, reflected in the exponential reduction of  $K_{ST}$ , demonstrates that runoff will be the dominant process for high fire severities, leading to reduced recharge rates. This highlights that groundwater recharge is highly sensitive to permeability reduction and canopy loss. Zomlot et al. [150] supported this statement, stating that the main factors contributing to recharge are vegetation cover, soil texture, and precipitation, in that specific order. In contrast, precipitation rates would be more critical in dry climates, where recharge becomes more sensitive to weather [65]. This also suggests that low foliage loss combined with soil not heavily altered by fire can lead to slightly higher recharge rates. This finding aligns with the new paradigm on the vegetation–recharge relationship [151,152], which indicates that groundwater recharge will be maximum for intermediate tree densities. This understanding is also important for informing the sustainable urban planning and management of natural resources in fire-prone areas, in support of SDG 11 (Sustainable cities and communities).

Less direct post-fire processes are associated with evapotranspiration rates, which are sensitive to on-site conditions and fire severity, turning into a dominant process for recharge under low to moderate fire scenarios. The changing dynamics of wildfires can lead to critical feedback in global and regional climates [36]. These changes are connected with evapotranspiration, a key process in basin-scale hydrology, controlling water availability under certain conditions. Around half of the typical yearly rainfall can be lost in tropical regions like the Amazon via evapotranspiration [153]. However, the increases in evaporation rates, together with the reduction in post-fire transpiration, make it challenging to determine the increase or reduction of fire-induced evapotranspiration. Moreover, the direct dependence on post-fire climate trends and a highly time-sensitive albedo hinder the prediction of evapotranspiration. Consequently, it is relevant to improve the comprehension of the microclimate after a fire and the projection of climatic variables included in recharge models.

### 5.1. Challenges and Advances in Measuring Wind Speed for Improved Post-Fire Evapotranspiration Estimation

The effect of fire on wind speed is relevant to explain possible changes in evapotranspiration (ET). Wind speed will increase after a wildfire, raising evaporation rates. Since its effect is directly related to vegetation reduction, transpiration could decrease just after the fire. Transpiration tends to return to its pre-fire values if the vegetation regenerates or is replaced. Furthermore, in the short term, it is also variable, as wind speed is quite dynamic even over short periods, and its correlation with burned areas varies seasonally. For ex-



ample, the combined effect of increased wind speeds with increased temperature would accentuate the evaporation process in winter. Experimental studies showed a correlation between burned area and wind velocity can be suppressed during the summer season [36]. This occurs because surface cooling driven by wind during times of high solar intensity may counteract the drying effect of increased wind speed [154]. The relationship between wind and forest fires is evident, dynamic, and codependent on other hydrometeorological variables, which strongly depend on vegetation cover.

Incorporating these changes into models requires accounting for wind speed, a significant variable affecting evapotranspiration. For instance, the Penman-Monteith method incorporates wind speed values into estimates of aerodynamic roughness, representing the resistance water vapor encounters when moving through specific land cover types. While the metric is well defined, data quality is often associated with uncertainty [36], potentially magnifying simulation inaccuracies for post-fire wind data. The actual values of wind velocity may not be reflected in meteorological databases. In forests, increased surface roughness and complex structure can partially dissociate wind velocity measurements within the canopy from those outside it [36,155]. As a result, measuring wind speeds in montane forests is more challenging compared to open landscapes with more accessible wind speed measurements. Some advancements offer approaches for obtaining more accurate wind speed data within forest canopies. While existing techniques in the literature aim to improve wind databases, further data acquisition is needed to enhance post-fire wind predictions.

### *5.2. Impacts of Wildfires on Surface Temperatures and Evapotranspiration in Forest Ecosystems*

The soil and understory vegetation cover beneath the forest canopy generally exhibit smaller temperature variations between day and night due to light absorption and evaporative cooling from transpiration. [156–161]. When this buffering effect is disrupted, combined with decreased albedo after a wildfire, it leads to higher surface temperatures and increased potential for heating soil and air [93,136,162,163]. This effect is primarily reflected in increased maximum surface temperatures, especially in coniferous forests covering soils with high water availability. Furthermore, this increase in maximum land temperature is most evident immediately after a wildfire during summer periods [164]. It diminishes over time as vegetation gradually regenerates. Consequently, changes in surface temperature become minimal and almost insignificant in the first years following a wildfire [88]. The logical consequence in the water balance includes increased evaporation and decreased soil moisture, reducing transpiration of damaged vegetation [161].

Temperature is a crucial variable widely used to estimate reference evapotranspiration (ET<sub>o</sub>), primarily due to the ease of its measurement and significant data availability. Various methods for calculating ET<sub>o</sub>, such as those of Thornthwaite, Hargreaves, and Turc, rely on empirical dependencies on temperature and are straightforward to compute. Other methods, like the Penman-Monteith, which is partly based on energy fluxes, use temperature as a proxy for atmospheric humidity [36]. The vapor pressure deficit (VPD), which is the difference between the saturation and actual vapor pressure, has garnered recent interest. Since it increases exponentially with temperature, it is easier to correlate it with different fire severities. However, given the difficulty in inferring future trends, VPD could emerge as an interesting alternative, as its sensitivity to fire has generated increasing interest [165].

Temperature and wind speed are essential factors influencing evapotranspiration, a water-balance component with substantial uncertainty. Vapor pressure deficit (VPD) has been proposed as an alternative, but its use remains subject to debate. Remote sensing-based corrections for forest wind velocity data are being promoted as a valuable option, particularly in areas lacking comprehensive hydrometeorological instrumentation. Further research is required to redefine sensitive metrics, enhance measurement quality, and calibrate models with independent data.

Post-fire microclimate research is an area that needs additional research. The challenges of predicting future trends are accentuated by the potential influence of global

warming and concurrent climate extremes on recharge. These interconnected processes impact not only water distribution but also raise the likelihood of fire occurrence, as depicted in Figure 3. The literature highlights the need to account for complex interactions among water-balance components when incorporating climatic factors into hydrological models in post-fire settings given that even in areas close to fire-prone zones, changes in temperature and other climatic variables cause a gradual redistribution of water [166]. Nevertheless, integrating significant climatic inputs into post-fire hydrological models remains a challenge.

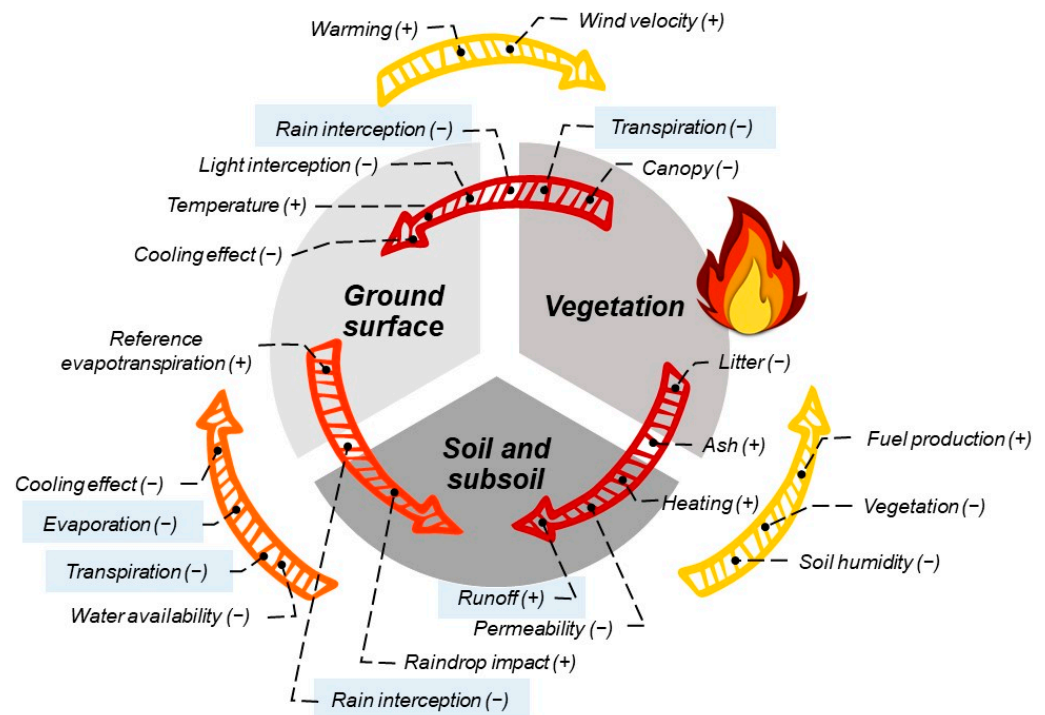


**Figure 3.** Schematic representation of the feedback mechanism between forest fire-impacted processes affecting water distribution. The figure emphasizes the sequential impacts on water-balance components, with a specific focus on the color (darker), highlighting the directness of the post-fire impact. The process begins with direct effects on vegetation and progresses to subsequent effects on soil and subsoil.

### 5.3. Harnessing Opportunities: Validation Alternatives with Satellite Insights and Neighboring Basin Analyses

The validation of hydrological models plays a crucial role in the accurate prediction of wildfire impacts on groundwater recharge [85]. Advanced satellite technologies like the Gravity Recovery and Climate Experiment (GRACE) offer comprehensive hydrological data [167–169] essential for the global-scale monitoring of hydrological dynamics and shifts in water storage, critical factors in understanding and predicting post-fire recovery processes. Furthermore, these satellite observations are indispensable for tracking fire-sensitive variables like the Leaf Area Index (LAI) and burn severity, offering refined inputs for hydrological models. These observations are crucial for understanding post-fire recovery processes, and incorporating advanced modeling techniques [170] enhances our ability to capture the dynamic changes in LAI post-fire, ensuring more accurate predictions of groundwater recharge in affected areas.

Employing neighboring basin studies for monitoring base flows significantly enhances model validation capabilities [171], particularly in regions affected by wildfires. Such studies not only enable multi-site validation but also allow for precise adjustments of model parameters, leveraging empirical data from areas that are ecologically similar yet differently affected by wildfires. [172]. Instrumenting burned basins to monitor recovery

processes such as transpiration in regenerating vegetation, sap flow, soil moisture, and albedo provides a deeper understanding of this dynamic recovery. This strategic approach is crucial for the effective management of water resources in regions recovering from wildfire disturbances.

## 6. Conclusions

The intuitive rationale behind physically based water-balance models has facilitated a deeper comprehension of the impacts of fire on individual hydrological processes. These models prove valuable in evaluating fire-induced alterations affecting groundwater recharge calculations as well as in examining the interconnectedness of these processes. The present analysis reveals several crucial knowledge and numerical gaps concerning post-fire recharge, particularly in relation to microclimatic conditions. Addressing these gaps is vital for enhancing our knowledge of the influence of fire on groundwater.

Currently, knowledge in this field can be applied to wildfire-prone areas to anticipate and mitigate the detrimental effects of fire on water availability. Numerous experimental studies have examined the impacts of fire on soil permeability and vegetation density parameters such as  $LAI$ ,  $CN$ , and  $K_{ST}$ . These parameters, cataloged for various post-fire periods, are primarily based on the  $DNBR$  metric, serving as the standard framework for post-fire hydrological research. Moreover, it is essential to extrapolate these parameters to a broader range of locations while advancements in remote sensing technology continue to enhance the accuracy of meteorological inputs.

Though simulating post-fire scenarios can be imprecise and uncertain, modeling remains the most effective decision-making tool for promoting sustainable water management. We now possess a wealth of published data on crucial hydrological parameters, a solid understanding of the variability of each hydrological component following a fire, and guidelines for implementing them through modeling. Evaluating the performance of these models will equip decision makers with the technical foundation necessary for the sustainable management of water resources in the context of changing land use. Incorporating refined strategies that integrate contemporary sustainable approaches can further enhance the management of wildfires and water resources, acknowledging the complex influence of human activities on ecological dynamics. As the use of post-fire simulations becomes more widespread, research on hydrological inputs under a broader range of conditions will be encouraged, and validation will become increasingly important, ultimately leading to improvements. This expanded research will encourage ongoing model validation and refinement, ultimately leading to significant improvements in our understanding and management of post-fire water dynamics.

**Author Contributions:** M.G.-R. led the conceptualization and methodology of this literature review, focusing on organizing and analyzing key research findings, and she crafted the initial draft, ensuring it clearly presented the accumulated knowledge in the field; J.F. improved the presentation of the review by refining the graphics and tables, which helped clarify complex information; P.d. managed the project's logistics and provided critical feedback on the manuscript, contributing to its overall coherence and quality; M.H. supervised the review process and played a key role in refining the content, offering detailed edits that enhanced the manuscript's academic quality. All authors have read and agreed to the published version of the manuscript.

**Funding:** This research has been funded by VLIR-UOS: Vlaamse Interuniversitaire Raad-Universitaire Ontwikkelingssamenwerking (Grant Number BO2017IUC034A105) and by the DGD: Directorate General for Development Cooperation and Humanitarian Aid.

**Data Availability Statement:** No new data were created or analyzed in this study. Data sharing is not applicable to this article.

**Acknowledgments:** We sincerely thank Josue Góngora for his skillful illustrations, which allowed us to incorporate aspects of the Chiquitania region's features. Located in eastern Bolivia, this area faces challenges from wildfires and water scarcity. We appreciate his warm, professional collaboration.

Additionally, we are profoundly thankful to Jeffrey Green for his prompt and thorough review of the English text, enhancing the clarity and readability of our work.

**Conflicts of Interest:** On behalf of all authors, the corresponding author states that there are no conflicts of interest.

## References

1. Westerling, A.L.; Hidalgo, H.G.; Cayan, D.R.; Swetnam, T.W. Warming and Earlier Spring Increase Western U.S. Forest Wildfire Activity. *Science* **2006**, *313*, 940–943. [[CrossRef](#)] [[PubMed](#)]
2. Flannigan, M.; Stocks, B.; Turetsky, M.; Wotton, M. Impacts of Climate Change on Fire Activity and Fire Management in the Circumboreal Forest. *Glob. Chang. Biol.* **2009**, *15*, 549–560. [[CrossRef](#)]
3. Bowman, D.M.J.S.; Balch, J.K.; Artaxo, P.; Bond, W.J.; Carlson, J.M.; Cochrane, M.A.; D’Antonio, C.M.; DeFries, R.S.; Doyle, J.C.; Harrison, S.P.; et al. Fire in the Earth System. *Science* **2009**, *324*, 481–484. [[CrossRef](#)] [[PubMed](#)]
4. Ward, D.S.; Kloster, S.; Mahowald, N.M.; Rogers, B.M.; Randerson, J.T.; Hess, P.G. The Changing Radiative Forcing of Fires: Global Model Estimates for Past, Present and Future. *Atmos. Chem. Phys.* **2012**, *12*, 10857–10886. [[CrossRef](#)]
5. Abatzoglou, J.T.; Williams, A.P. Impact of Anthropogenic Climate Change on Wildfire across Western US Forests. *Proc. Natl. Acad. Sci. USA* **2016**, *113*, 11770–11775. [[CrossRef](#)] [[PubMed](#)]
6. Williams, C.H.S.; Silins, U.; Spencer, S.A.; Wagner, M.J.; Stone, M.; Emelko, M.B.; Williams, C.H.S.; Silins, U.; Spencer, S.A.; Wagner, M.J.; et al. Net Precipitation in Burned and Unburned Subalpine Forest Stands after Wildfire in the Northern Rocky Mountains. *Int. J. Wildland Fire* **2019**, *28*, 750–760. [[CrossRef](#)]
7. Zhao, Y.; Zhang, M.; Liu, Z.; Ma, J.; Yang, F.; Guo, H.; Fu, Q. How Human Activities Affect Groundwater Storage. *Research* **2024**, *7*, 0369. [[CrossRef](#)]
8. Gillett, N.P.; Weaver, A.J.; Zwiers, F.W.; Flannigan, M.D. Detecting the Effect of Climate Change on Canadian Forest Fires. *Geophys. Res. Lett.* **2004**, *31*. [[CrossRef](#)]
9. Brando, P.M.; Soares-Filho, B.; Rodrigues, L.; Assunção, A.; Morton, D.; Tuchsneider, D.; Fernandes, E.C.M.; Macedo, M.N.; Oliveira, U.; Coe, M.T. The Gathering Firestorm in Southern Amazonia. *Sci. Adv.* **2020**, *6*, eaay1632. [[CrossRef](#)]
10. Bustillo Sánchez, M.; Tonini, M.; Mapelli, A.; Fiorucci, P. Spatial Assessment of Wildfires Susceptibility in Santa Cruz (Bolivia) Using Random Forest. *Geosciences* **2021**, *11*, 224. [[CrossRef](#)]
11. Maillard, O.; Vides-Almonacid, R.; Flores-Valencia, M.; Coronado, R.; Vogt, P.; Vicente-Serrano, S.M.; Azurduy, H.; Anívarro, R.; Cuellar, R.L. Relationship of Forest Cover Fragmentation and Drought with the Occurrence of Forest Fires in the Department of Santa Cruz, Bolivia. *Forests* **2020**, *11*, 910. [[CrossRef](#)]
12. Adams, M.A. Mega-Fires, Tipping Points and Ecosystem Services: Managing Forests and Woodlands in an Uncertain Future. *For. Ecol. Manag.* **2013**, *294*, 250–261. [[CrossRef](#)]
13. Dudley, N.; Stolton, S. *Running Pure the Importance of Forest Protected Areas to Drinking Water*; World Bank/WWF Alliance for Forest Conservation and Sustainable Use: Washington, DC, USA, 2013; ISBN 978-2-88085-262-7.
14. Fienen, M.N.; Arshad, M. The International Scale of the Groundwater Issue. In *Integrated Groundwater Management: Concepts, Approaches and Challenges*; Jakeman, A.J., Barreteau, O., Hunt, R.J., Rinaudo, J.-D., Ross, A., Eds.; Springer International Publishing: Cham, Switzerland, 2016; pp. 21–48, ISBN 978-3-319-23576-9.
15. Foster, S.; Chilton, J.; Moeng, M.; Cardy, F.; Schiffler, M. *Groundwater in Rural Development*; The World Bank: Washington, DC, USA, 2000; ISBN 978-0-8213-4703-4.
16. MacDonald, A.; Calow, R. Developing Groundwater for Secure Rural Water Supplies in Africa. *Desalination* **2008**, *248*, 546–556. [[CrossRef](#)]
17. Chaminé, H.I.; Carvalho, J.M.; Freitas, L. Sustainable Groundwater Management in Rural Communities in Developed Countries: Some Thoughts and Outlook. *Mediterr. Geosci. Rev.* **2021**, *3*, 389–398. [[CrossRef](#)]
18. Taylor, R.G.; Scanlon, B.; Döll, P.; Rodell, M.; van Beek, R.; Wada, Y.; Longuevergne, L.; Leblanc, M.; Famiglietti, J.S.; Edmunds, M.; et al. Ground Water and Climate Change. *Nat. Clim. Chang.* **2013**, *3*, 322–329. [[CrossRef](#)]
19. Shahid, S.; Alamgir, M.; Wang, X.; Eslamian, S. Climate Change Impacts on and Adaptation to Groundwater. In *Handbook of Drought and Water Scarcity*; CRC Press: Boca Raton, FL, USA, 2017; ISBN 978-1-315-22678-1.
20. Adane, Z.; Zlotnik, V.A.; Rossman, N.R.; Wang, T.; Nasta, P. Sensitivity of Potential Groundwater Recharge to Projected Climate Change Scenarios: A Site-Specific Study in the Nebraska Sand Hills, USA. *Water* **2019**, *11*, 950. [[CrossRef](#)]
21. Han, Q.; Qi, T.; Khanaum, M.M. Evaluation of the Offsets of Artificial Recharge on the Extra Run-Off Induced by Urbanization and Extreme Storms Based on an Enhanced Semi-Distributed Hydrologic Model with an Infiltration Basin Module. *Water* **2024**, *16*, 1032. [[CrossRef](#)]
22. Cartwright, J.; Johnson, H.M. Springs as Hydrologic Refugia in a Changing Climate? A Remote-Sensing Approach. *Ecosphere* **2018**, *9*, e02155. [[CrossRef](#)]
23. Fan, L.; Wang, J.; Zhao, Y.; Wang, X.; Mo, K.; Li, M. Reconstructing 273 Years of Potential Groundwater Recharge Dynamics in a Near-Humid Monsoon Loess Unsaturated Zone Using Chloride Profiling. *Water* **2024**, *16*, 2147. [[CrossRef](#)]
24. Barry, R.; Barbecot, F.; Rodriguez, M.; Mattéi, A.; Djongon, A. Estimating Climate Change’s Impacts on the Recharge of an Ungauged Tropical Aquifer (Togolese Coastal Sedimentary Basin). *Water* **2024**, *16*, 731. [[CrossRef](#)]



25. Ferreira, A.J.D.; Coelho, C.O.A.; Ritsema, C.J.; Boulet, A.K.; Keizer, J.J. Soil and Water Degradation Processes in Burned Areas: Lessons Learned from a Nested Approach. *Catena* **2008**, *74*, 273–285. [[CrossRef](#)]
26. Mansilha, C.; Carvalho, A.; Guimaraes, P.; Espinha Marques, J. Effects of Forest Fires on Groundwater Contamination. In Proceedings of the IWA World Water Congress & Exhibition, Lisbon, Portugal, 21–26 September 2014.
27. Li, J.; Pang, Z.; Liu, Y.; Hu, S.; Jiang, W.; Tian, L.; Yang, G.; Jiang, Y.; Jiao, X.; Tian, J. Changes in Groundwater Dynamics and Geochemical Evolution Induced by Drainage Reorganization: Evidence from 81Kr and 36Cl Dating of Geothermal Water in the Weihe Basin of China. *Earth Planet. Sci. Lett.* **2023**, *623*, 118425. [[CrossRef](#)]
28. Kazakis, N.; Karakatsanis, D.; Ntona, M.M.; Polydoropoulos, K.; Zavridou, E.; Voudouri, K.A.; Busico, G.; Kalaitzidou, K.; Patsialis, T.; Perdikaki, M.; et al. Groundwater Depletion. Are Environmentally Friendly Energy Recharge Dams a Solution? *Water* **2024**, *16*, 1541. [[CrossRef](#)]
29. Emelko, M.B.; Silins, U.; Bladon, K.D.; Stone, M. Implications of Land Disturbance on Drinking Water Treatability in a Changing Climate: Demonstrating the Need for “Source Water Supply and Protection” Strategies. *Water Res.* **2011**, *45*, 461–472. [[CrossRef](#)] [[PubMed](#)]
30. Morales García, R.; Ruiz Hernández, J.M.; Orden Gómez, J.A.d.l.; Gómez Gómez, J.d.D.; Moreno Merino, L.; Domínguez Sánchez, J.A.; García Bravo, N.; Durán Valsero, J.J. *Incendios Forestales y Aguas Subterráneas: Un Análisis de los Efectos Ambientales y Económicos Sobre los Acuíferos*; CSIC—Instituto Geológico y Minero de España (IGME): Madrid, Spain, 2020.
31. Xu, Z.; Zhang, Y.; Zhang, X.; Ma, N.; Tian, J.; Kong, D.; Post, D. Bushfire-Induced Water Balance Changes Detected by a Modified Paired Catchment Method. *Water Resour. Res.* **2022**, *58*, e2021WR031013. [[CrossRef](#)]
32. Shakesby, R.A.; Doerr, S.H. Wildfire as a Hydrological and Geomorphological Agent. *Earth-Sci. Rev.* **2006**, *74*, 269–307. [[CrossRef](#)]
33. Rodrigues, E.L.; Jacobi, C.M.; Figueira, J.E.C. Wildfires and Their Impact on the Water Supply of a Large Neotropical Metropolis: A Simulation Approach. *Sci. Total Environ.* **2019**, *651*, 1261–1271. [[CrossRef](#)]
34. Johnk, B.T.; Mays, D.C. Wildfire Impacts on Groundwater Aquifers: A Case Study of the 1996 Honey Boy Fire in Beaver County, Utah, USA. *Water* **2021**, *13*, 2279. [[CrossRef](#)]
35. Wine, M.L.; Cadol, D. Hydrologic Effects of Large Southwestern USA Wildfires Significantly Increase Regional Water Supply: Fact or Fiction? *Environ. Res. Lett.* **2016**, *11*, 085006. [[CrossRef](#)]
36. Williams, A.P.; Seager, R.; Berkelhammer, M.; Macalady, A.K.; Crimmins, M.A.; Swetnam, T.W.; Trugman, A.T.; Buening, N.; Hryniw, N.; McDowell, N.G.; et al. Causes and Implications of Extreme Atmospheric Moisture Demand during the Record-Breaking 2011 Wildfire Season in the Southwestern United States. *J. Appl. Meteorol. Climatol.* **2014**, *53*, 2671–2684. [[CrossRef](#)]
37. Neary, D.G.; Ryan, K.C.; DeBano, L.F. (Eds.) *Wildland Fire in Ecosystems: Effects of Fire on Soils and Water*. In *General Technical Report RMRS-GTR-42. Volume 4*; U.S. Department of Agriculture, Forest Service, Rocky Mountain Research Station: Ogden, UT, USA, 2005; 250p. [[CrossRef](#)]
38. Smith, H.G.; Sheridan, G.J.; Lane, P.N.J.; Nyman, P.; Haydon, S. Wildfire Effects on Water Quality in Forest Catchments: A Review with Implications for Water Supply. *J. Hydrol.* **2011**, *396*, 170–192. [[CrossRef](#)]
39. Dahm, C.N.; Candelaria-Ley, R.I.; Reale, C.S.; Reale, J.K.; Horn, D.J.V. Extreme Water Quality Degradation Following a Catastrophic Forest Fire. *Freshw. Biol.* **2015**, *60*, 2584–2599. [[CrossRef](#)]
40. Reale, J.K.; Van Horn, D.J.; Condon, K.E.; Dahm, C.N. The Effects of Catastrophic Wildfire on Water Quality along a River Continuum. *Freshw. Sci.* **2015**, *34*, 1426–1442. [[CrossRef](#)]
41. Emmerton, C.A.; Cooke, C.A.; Hustins, S.; Silins, U.; Emelko, M.B.; Lewis, T.; Kruk, M.K.; Taube, N.; Zhu, D.; Jackson, B.; et al. Severe Western Canadian Wildfire Affects Water Quality Even at Large Basin Scales. *Water Res.* **2020**, *183*, 116071. [[CrossRef](#)]
42. Moody, J.A.; Martin, D.A.; Haire, S.L.; Kinner, D.A. Linking Runoff Response to Burn Severity after a Wildfire. *Hydrol. Process.* **2008**, *22*, 2063–2074. [[CrossRef](#)]
43. Ebel, B.A.; Moody, J.A. Rethinking Infiltration in Wildfire-Affected Soils. *Hydrol. Process.* **2013**, *27*, 1510–1514. [[CrossRef](#)]
44. Poon, P.K.; Kinoshita, A.M. Estimating Evapotranspiration in a Post-Fire Environment Using Remote Sensing and Machine Learning. *Remote Sens.* **2018**, *10*, 1728. [[CrossRef](#)]
45. Williams, A.P.; Livneh, B.; McKinnon, K.A.; Hansen, W.D.; Mankin, J.S.; Cook, B.I.; Smerdon, J.E.; Varuolo-Clarke, A.M.; Bjarke, N.R.; Juang, C.S.; et al. Growing Impact of Wildfire on Western US Water Supply. *Proc. Natl. Acad. Sci. USA* **2022**, *119*, e2114069119. [[CrossRef](#)]
46. Ryan, S.E. Impacts of Wildfire on Runoff and Sediment Loads at Little Granite Creek, Western Wyoming. *Geomorphology* **2011**, *129*, 113–130. [[CrossRef](#)]
47. Shakesby, R.A. Post-Wildfire Soil Erosion in the Mediterranean: Review and Future Research Directions. *Earth-Sci. Rev.* **2011**, *105*, 71–100. [[CrossRef](#)]
48. Ebel, B.A.; Rengers, F.K.; Tucker, G.E. Observed and Simulated Hydrologic Response for a First-Order Catchment during Extreme Rainfall 3 Years after Wildfire Disturbance. *Water Resour. Res.* **2016**, *52*, 9367–9389. [[CrossRef](#)]
49. Cole, R.P.; Bladon, K.D.; Wagenbrenner, J.W.; Coe, D.B.R. Hillslope Sediment Production after Wildfire and Post-Fire Forest Management in Northern California. *Hydrol. Process.* **2020**, *34*, 5242–5259. [[CrossRef](#)]
50. Tetzlaff, D.; Carey, S.K.; McNamara, J.P.; Laudon, H.; Soulsby, C. The Essential Value of Long-Term Experimental Data for Hydrology and Water Management. *Water Resour. Res.* **2017**, *53*, 2598–2604. [[CrossRef](#)]
51. Atchley, A.L.; Kinoshita, A.M.; Lopez, S.R.; Trader, L.; Middleton, R. Simulating Surface and Subsurface Water Balance Changes Due to Burn Severity. *Vadose Zone J.* **2018**, *17*, 180099. [[CrossRef](#)]



52. Batelis, S.-C.; Nalbantis, I. Potential Effects of Forest Fires on Streamflow in the Enipeas River Basin, Thessaly, Greece. *Environ. Process.* **2014**, *1*, 73–85. [[CrossRef](#)]
53. Soulis, K.X. Estimation of SCS Curve Number Variation Following Forest Fires. *Hydrol. Sci. J.* **2018**, *63*, 1332–1346. [[CrossRef](#)]
54. Venkatesh, K.; Preethi, K.; Ramesh, H. Evaluating the Effects of Forest Fire on Water Balance Using Fire Susceptibility Maps. *Ecol. Indic.* **2020**, *110*, 105856. [[CrossRef](#)]
55. Soto, B.; Diaz-Fierros, F. Soil Water Balance as Affected by Throughfall in Gorse (*Ulex europaeus*, L.) Shrubland after Burning. *J. Hydrol.* **1997**, *195*, 218–231. [[CrossRef](#)]
56. Silva, J.S.; Vaz, P.; Moreira, F.; Catry, F.; Rego, F.C. Wildfires as a Major Driver of Landscape Dynamics in Three Fire-Prone Areas of Portugal. *Landsc. Urban Plan.* **2011**, *101*, 349–358. [[CrossRef](#)]
57. Bellot, J.; Bonet, A.; Sanchez, J.R.; Chirino, E. Likely Effects of Land Use Changes on the Runoff and Aquifer Recharge in a Semiarid Landscape Using a Hydrological Model. *Landsc. Urban Plan.* **2001**, *55*, 41–53. [[CrossRef](#)]
58. Cardenas, M.B. Soil Moisture Variation and Dynamics across a Wildfire Burn Boundary in a Loblolly Pine (*Pinus taeda*) Forest. *J. Hydrol.* **2014**, *519*, 490–502. [[CrossRef](#)]
59. Ebel, B.A. Simulated Unsaturated Flow Processes after Wildfire and Interactions with Slope Aspect. *Water Resour. Res.* **2013**, *49*, 8090–8107. [[CrossRef](#)]
60. Batelaan, O.; De Smedt, F. GIS-Based Recharge Estimation by Coupling Surface–Subsurface Water Balances. *J. Hydrol.* **2007**, *337*, 337–355. [[CrossRef](#)]
61. Griebler, C.; Avramov, M. Groundwater Ecosystem Services: A Review. *Freshw. Sci.* **2015**, *34*, 355–367. [[CrossRef](#)]
62. Singh, A.; Panda, S.N.; Uzokwe, V.N.E.; Krause, P. An Assessment of Groundwater Recharge Estimation Techniques for Sustainable Resource Management. *Groundw. Sustain. Dev.* **2019**, *9*, 100218. [[CrossRef](#)]
63. Fernandez, J.; Maillard, O.; Uyuni, G.; Guzmán Rojo, M.X.; Escobar, M. Multi-Criteria Prioritization of Watersheds for Post-Fire Restoration Using GIS Tools and Google Earth Engine: A Case Study from the Department of Santa Cruz, Bolivia. *Water* **2023**, *15*, 3545. [[CrossRef](#)]
64. Jost, G.; Schume, H.; Hager, H. Factors Controlling Soil Water-Recharge in a Mixed European Beech (*Fagus sylvatica* L.)–Norway Spruce [*Picea abies* (L.) Karst.] Stand. *Eur. J. For. Res.* **2004**, *123*, 93–104. [[CrossRef](#)]
65. Scanlon, B.R.; Healy, R.W.; Cook, P.G. Choosing Appropriate Techniques for Quantifying Groundwater Recharge. *Hydrogeol. J.* **2002**, *10*, 18–39. [[CrossRef](#)]
66. Costa, M.H.; Foley, J.A. Water Balance of the Amazon Basin: Dependence on Vegetation Cover and Canopy Conductance. *J. Geophys. Res. Atmos.* **1997**, *102*, 23973–23989. [[CrossRef](#)]
67. Sun, Z.; Wei, B.; Su, W.; Shen, W.; Wang, C.; You, D.; Liu, Z. Evapotranspiration Estimation Based on the SEBAL Model in the Nansi Lake Wetland of China. *Math. Comput. Model.* **2011**, *54*, 1086–1092. [[CrossRef](#)]
68. Hornbeck, J.W.; Adams, M.B.; Corbett, E.S.; Verry, E.S.; Lynch, J.A. Long-Term Impacts of Forest Treatments on Water Yield: A Summary for Northeastern USA. *J. Hydrol.* **1993**, *150*, 323–344. [[CrossRef](#)]
69. Stednick, J.D. Monitoring the Effects of Timber Harvest on Annual Water Yield. *J. Hydrol.* **1996**, *176*, 79–95. [[CrossRef](#)]
70. Ellison, D.; Futter, M.N.; Bishop, K. On the Forest Cover–Water Yield Debate: From Demand- to Supply-Side Thinking. *Glob. Chang. Biol.* **2012**, *18*, 806–820. [[CrossRef](#)]
71. Miralles, D.G.; Teuling, A.J.; van Heerwaarden, C.C.; Vilà-Guerau de Arellano, J. Mega-Heatwave Temperatures Due to Combined Soil Desiccation and Atmospheric Heat Accumulation. *Nat. Geosci.* **2014**, *7*, 345–349. [[CrossRef](#)]
72. Anderegg, W.R.L.; Konings, A.G.; Trugman, A.T.; Yu, K.; Bowling, D.R.; Gabbitas, R.; Karp, D.S.; Pacala, S.; Sperry, J.S.; Sulman, B.N.; et al. Hydraulic Diversity of Forests Regulates Ecosystem Resilience during Drought. *Nature* **2018**, *561*, 538–541. [[CrossRef](#)]
73. Yang, X.; Zhang, K.; Chang, T.; Shaghaleh, H.; Qi, Z.; Zhang, J.; Ye, H.; Hamoud, Y.A. Interactive Effects of Microbial Fertilizer and Soil Salinity on the Hydraulic Properties of Salt-Affected Soil. *Plants* **2024**, *13*, 473. [[CrossRef](#)]
74. Bladon, K.D.; Emelko, M.B.; Silins, U.; Stone, M. Wildfire and the Future of Water Supply. *Environ. Sci. Technol.* **2014**, *48*, 8936–8943. [[CrossRef](#)]
75. Mills, A.J.; Fey, M.V. Frequent Fires Intensify Soil Crusting: Physicochemical Feedback in the Pedoderm of Long-Term Burn Experiments in South Africa. *Geoderma* **2004**, *121*, 45–64. [[CrossRef](#)]
76. Scott, D.F.; Van Wyk, D.B. The Effects of Wildfire on Soil Wettability and Hydrological Behaviour of an Afforested Catchment. *J. Hydrol.* **1990**, *121*, 239–256. [[CrossRef](#)]
77. Veraverbeke, S.; Lhermitte, S.; Verstraeten, W.W.; Goossens, R. The Temporal Dimension of Differenced Normalized Burn Ratio (dNBR) Fire/Burn Severity Studies: The Case of the Large 2007 Peloponnese Wildfires in Greece. *Remote Sens. Environ.* **2010**, *114*, 2548–2563. [[CrossRef](#)]
78. Hallema, D.W.; Robinne, F.-N.; Bladon, K.D. Reframing the Challenge of Global Wildfire Threats to Water Supplies. *Earths Future* **2018**, *6*, 772–776. [[CrossRef](#)]
79. Abatzoglou, J.T.; Kolden, C.A. Relationships between Climate and Macroscale Area Burned in the Western United States. *Int. J. Wildland Fire* **2013**, *22*, 1003–1020. [[CrossRef](#)]
80. Boisramé, G.; Thompson, S.; Collins, B.; Stephens, S. Managed Wildfire Effects on Forest Resilience and Water in the Sierra Nevada. *Ecosystems* **2017**, *20*, 717–732. [[CrossRef](#)]
81. Moody, J.A.; Shakesby, R.A.; Robichaud, P.R.; Cannon, S.H.; Martin, D.A. Current Research Issues Related to Post-Wildfire Runoff and Erosion Processes. *Earth-Sci. Rev.* **2013**, *122*, 10–37. [[CrossRef](#)]

82. Chen, F.; Warner, T.T.; Manning, K. Sensitivity of Orographic Moist Convection to Landscape Variability: A Study of the Buffalo Creek, Colorado, Flash Flood Case of 1996. *J. Atmos. Sci.* **2001**, *58*, 3204–3223. [[CrossRef](#)]
83. Moody, J.A.; Ebel, B.A. Hyper-Dry Conditions Provide New Insights into the Cause of Extreme Floods after Wildfire. *Catena* **2012**, *93*, 58–63. [[CrossRef](#)]
84. Kinoshita, A.M.; Hogue, T.S. Increased Dry Season Water Yield in Burned Watersheds in Southern California. *Environ. Res. Lett.* **2015**, *10*, 014003. [[CrossRef](#)]
85. Wagenbrenner, J.W.; Ebel, B.A.; Bladon, K.D.; Kinoshita, A.M. Post-Wildfire Hydrologic Recovery in Mediterranean Climates: A Systematic Review and Case Study to Identify Current Knowledge and Opportunities. *J. Hydrol.* **2021**, *602*, 126772. [[CrossRef](#)]
86. de Groen, M.M. *Modelling Interception and Transpiration at Monthly Time Steps: IHE Dissertation 31*; CRC Press: Boca Raton, FL, USA, 2002; ISBN 978-90-5809-378-3.
87. Cerdà, A.; Bodí, M.B.; Lasanta, T.; Mataix-Solera, J.; Doerr, S. Efectos de los incendios forestales sobre los suelos en España. El estado de la cuestión visto por los científicos españoles. In *Cátedra de Divulgación de la Ciencia*; Universitat de Valencia: Valencia, Spain, 2009; pp. 355–383, ISBN 978-84-370-7653-9.
88. Veraverbeke, S.; Verstraeten, W.W.; Lhermitte, S.; Kerchove, R.V.D.; Goossens, R.; Veraverbeke, S.; Verstraeten, W.W.; Lhermitte, S.; Kerchove, R.V.D.; Goossens, R. Assessment of Post-Fire Changes in Land Surface Temperature and Surface Albedo, and Their Relation with Fire–Burn Severity Using Multitemporal MODIS Imagery. *Int. J. Wildland Fire* **2012**, *21*, 243–256. [[CrossRef](#)]
89. Bremer, D.J.; Ham, J.M. Effect of Spring Burning on the Surface Energy Balance in a Tallgrass Prairie. *Agric. For. Meteorol.* **1999**, *97*, 43–54. [[CrossRef](#)]
90. Beringer, J.; Hutley, L.B.; Tapper, N.J.; Coutts, A.; Kerley, A.; O’Grady, A.P. Fire Impacts on Surface Heat, Moisture and Carbon Fluxes from a Tropical Savanna in Northern Australia. *Int. J. Wildland Fire* **2003**, *12*, 333–340. [[CrossRef](#)]
91. Amiro, B.D.; Orchansky, A.L.; Barr, A.G.; Black, T.A.; Chambers, S.D.; Chapin, F.S., III; Goulden, M.L.; Litvak, M.; Liu, H.P.; McCaughy, J.H.; et al. The Effect of Post-Fire Stand Age on the Boreal Forest Energy Balance. *Agric. For. Meteorol.* **2006**, *140*, 41–50. [[CrossRef](#)]
92. Wendt, C.K.; Beringer, J.; Tapper, N.J.; Hutley, L.B. Local Boundary-Layer Development over Burnt and Unburnt Tropical Savanna: An Observational Study. *Bound.-Layer Meteorol.* **2007**, *124*, 291–304. [[CrossRef](#)]
93. Tsuyuzaki, S.; Kushida, K.; Kodama, Y. Recovery of Surface Albedo and Plant Cover after Wildfire in a Picea Mariana Forest in Interior Alaska. *Clim. Chang.* **2008**, *93*, 517–525. [[CrossRef](#)]
94. *FAO The State of Food and Agriculture 2020: Overcoming Water Challenges in Agriculture*; The State of Food and Agriculture (SOFA); FAO: Rome, Italy, 2020; ISBN 978-92-5-133441-6.
95. Zema, D.A. Postfire Management Impacts on Soil Hydrology. *Curr. Opin. Environ. Sci. Health* **2021**, *21*, 100252. [[CrossRef](#)]
96. Ichoku, C.; Ellison, L.T.; Willmot, K.E.; Matsui, T.; Dezfuli, A.K.; Gatebe, C.K.; Wang, J.; Wilcox, E.M.; Lee, J.; Adegoke, J.; et al. Biomass Burning, Land-Cover Change, and the Hydrological Cycle in Northern Sub-Saharan Africa. *Environ. Res. Lett.* **2016**, *11*, 095005. [[CrossRef](#)]
97. Certini, G. Effects of Fire on Properties of Forest Soils: A Review. *Oecologia* **2005**, *143*, 1–10. [[CrossRef](#)]
98. Cerdà, A.; Doerr, S.H. The Effect of Ash and Needle Cover on Surface Runoff and Erosion in the Immediate Post-Fire Period. *Catena* **2008**, *74*, 256–263. [[CrossRef](#)]
99. Larsen, I.J.; MacDonald, L.H.; Brown, E.; Rough, D.; Welsh, M.J.; Pietraszek, J.H.; Libohova, Z.; de Dios Benavides-Solorio, J.; Schaffrath, K. Causes of Post-Fire Runoff and Erosion: Water Repellency, Cover, or Soil Sealing? *Soil Sci. Soc. Am. J.* **2009**, *73*, 1393–1407. [[CrossRef](#)]
100. Balfour, V.N.; Doerr, S.H.; Robichaud, P.R. The Temporal Evolution of Wildfire Ash and Implications for Post-Fire Infiltration. *Int. J. Wildland Fire* **2014**, *23*, 733–745. [[CrossRef](#)]
101. Pereira, P.; Francos, M.; Brevik, E.C.; Ubeda, X.; Bogunovic, I. Post-Fire Soil Management. *Curr. Opin. Environ. Sci. Health* **2018**, *5*, 26–32. [[CrossRef](#)]
102. Sheridan, G.J.; Lane, P.N.J.; Noske, P.J. Quantification of Hillslope Runoff and Erosion Processes before and after Wildfire in a Wet Eucalyptus Forest. *J. Hydrol.* **2007**, *343*, 12–28. [[CrossRef](#)]
103. Cawson, J.G.; Sheridan, G.J.; Smith, H.G.; Lane, P.N.J. Effects of Fire Severity and Burn Patchiness on Hillslope-Scale Surface Runoff, Erosion and Hydrologic Connectivity in a Prescribed Burn. *For. Ecol. Manag.* **2013**, *310*, 219–233. [[CrossRef](#)]
104. Stoof, C.R.; Ferreira, A.J.D.; Mol, W.; Van den Berg, J.; De Kort, A.; Drooger, S.; Slingerland, E.C.; Mansholt, A.U.; Ferreira, C.S.S.; Ritsema, C.J. Soil Surface Changes Increase Runoff and Erosion Risk after a Low–Moderate Severity Fire. *Geoderma* **2015**, *239–240*, 58–67. [[CrossRef](#)]
105. DeBano, L.F. The Role of Fire and Soil Heating on Water Repellency in Wildland Environments: A Review. *J. Hydrol.* **2000**, *231–232*, 195–206. [[CrossRef](#)]
106. Smith, J.L.; Halvorson, J.J.; Bolton, H. Soil Properties and Microbial Activity across a 500m Elevation Gradient in a Semi-Arid Environment. *Soil Biol. Biochem.* **2002**, *34*, 1749–1757. [[CrossRef](#)]
107. Balfour, V.N.; Woods, S.W. The Hydrological Properties and the Effects of Hydration on Vegetative Ash from the Northern Rockies, USA. *Catena* **2013**, *111*, 9–24. [[CrossRef](#)]
108. Moody, J.A.; Ebel, B.A.; Nyman, P.; Martin, D.A.; Stoof, C.; McKinley, R.; Moody, J.A.; Ebel, B.A.; Nyman, P.; Martin, D.A.; et al. Relations between Soil Hydraulic Properties and Burn Severity. *Int. J. Wildland Fire* **2015**, *25*, 279–293. [[CrossRef](#)]

109. Ebel, B.A.; Moody, J.A. Parameter Estimation for Multiple Post-Wildfire Hydrologic Models. *Hydrol. Process.* **2020**, *34*, 4049–4066. [[CrossRef](#)]
110. Ebel, B.A.; Moody, J.A. Synthesis of Soil-Hydraulic Properties and Infiltration Timescales in Wildfire-Affected Soils. *Hydrol. Process.* **2017**, *31*, 324–340. [[CrossRef](#)]
111. Key, C.H.; Benson, N.C. Landscape Assessment (LA). In *FIREMON: Fire Effects Monitoring and Inventory System*; U.S. Department of Agriculture, Forest Service, Rocky Mountain Research Station: Fort Collins, CO, USA, 2006; pp. 1–55.
112. Salem, A.M.M. A Fully Distributed Integrated Hydrologic Model for Integrated Water Resources Management in a Highly Regulated River Floodplain. Ph.D. Thesis, University of Pecs, Pecs, Hungary, 2022.
113. Mastrotheodoros, T.; Pappas, C.; Molnar, P.; Burlando, P.; Manoli, G.; Parajka, J.; Rigon, R.; Szeles, B.; Bottazzi, M.; Hadjidoukas, P.; et al. More Green and Less Blue Water in the Alps during Warmer Summers. *Nat. Clim. Chang.* **2020**, *10*, 155–161. [[CrossRef](#)]
114. Finch, J.W. Estimating Change in Direct Groundwater Recharge Using a Spatially Distributed Soil Water Balance Model. *Q. J. Eng. Geol. Hydrogeol.* **2001**, *34*, 71–83. [[CrossRef](#)]
115. van Wagtenonk, J.W.; Root, R.R.; Key, C.H. Comparison of AVIRIS and Landsat ETM+ Detection Capabilities for Burn Severity. *Remote Sens. Environ.* **2004**, *92*, 397–408. [[CrossRef](#)]
116. Lentile, L.B.; Holden, Z.A.; Smith, A.M.S.; Falkowski, M.J.; Hudak, A.T.; Morgan, P.; Lewis, S.A.; Gessler, P.E.; Benson, N.C.; Lentile, L.B.; et al. Remote Sensing Techniques to Assess Active Fire Characteristics and Post-Fire Effects. *Int. J. Wildland Fire* **2006**, *15*, 319–345. [[CrossRef](#)]
117. Heward, H.; Smith, A.M.S.; Roy, D.P.; Tinkham, W.T.; Hoffman, C.M.; Morgan, P.; Lannom, K.O.; Heward, H.; Smith, A.M.S.; Roy, D.P.; et al. Is Burn Severity Related to Fire Intensity? Observations from Landscape Scale Remote Sensing. *Int. J. Wildland Fire* **2013**, *22*, 910–918. [[CrossRef](#)]
118. Parks, S.A.; Holsinger, L.M.; Panunto, M.H.; Jolly, W.M.; Dobrowski, S.Z.; Dillon, G.K. High-Severity Fire: Evaluating Its Key Drivers and Mapping Its Probability across Western US Forests. *Environ. Res. Lett.* **2018**, *13*, 044037. [[CrossRef](#)]
119. Smith, A.M.S.; Wooster, M.J.; Smith, A.M.S.; Wooster, M.J. Remote Classification of Head and Backfire Types from MODIS Fire Radiative Power and Smoke Plume Observations. *Int. J. Wildland Fire* **2005**, *14*, 249–254. [[CrossRef](#)]
120. Keeley, J.E.; Brennan, T.; Pfaff, A.H. Fire Severity and Ecosystem Responses Following Crown Fires in California Shrublands. *Ecol. Appl.* **2008**, *18*, 1530–1546. [[CrossRef](#)]
121. Adams, H.D.; Luce, C.H.; Breshears, D.D.; Allen, C.D.; Weiler, M.; Hale, V.C.; Smith, A.M.S.; Huxman, T.E. Ecohydrological Consequences of Drought- and Infestation- Triggered Tree Die-off: Insights and Hypotheses. *Ecohydrology* **2012**, *5*, 145–159. [[CrossRef](#)]
122. Cocke, A.E.; Fulé, P.Z.; Crouse, J.E. Comparison of Burn Severity Assessments Using Differenced Normalized Burn Ratio and Ground Data. *Int. J. Wildland Fire* **2005**, *14*, 189–198. [[CrossRef](#)]
123. Epting, J.; Verbyla, D.; Sorbel, B. Evaluation of Remotely Sensed Indices for Assessing Burn Severity in Interior Alaska Using Landsat TM and ETM+. *Remote Sens. Environ.* **2005**, *96*, 328–339. [[CrossRef](#)]
124. French, N.H.F.; Kasischke, E.S.; Hall, R.J.; Murphy, K.A.; Verbyla, D.L.; Hoy, E.E.; Allen, J.L.; French, N.H.F.; Kasischke, E.S.; Hall, R.J.; et al. Using Landsat Data to Assess Fire and Burn Severity in the North American Boreal Forest Region: An Overview and Summary of Results. *Int. J. Wildland Fire* **2008**, *17*, 443–462. [[CrossRef](#)]
125. Wells, C.G. *Effects of Fire on Soil: A State-of-Knowledge Review*; Department of Agriculture, Forest Service: Washington, DC, USA, 1979.
126. Holden, Z.A.; Morgan, P.; Evans, J.S. A Predictive Model of Burn Severity Based on 20-Year Satellite-Inferred Burn Severity Data in a Large Southwestern US Wilderness Area. *For. Ecol. Manag.* **2009**, *258*, 2399–2406. [[CrossRef](#)]
127. de Benavides-Solorio, J.D.; MacDonald, L.H. Measurement and Prediction of Post-Fire Erosion at the Hillslope Scale, Colorado Front Range. *Int. J. Wildland Fire* **2005**, *14*, 457–474. [[CrossRef](#)]
128. Vieira, D.C.S.; Fernández, C.; Vega, J.A.; Keizer, J.J. Does Soil Burn Severity Affect the Post-Fire Runoff and Interrill Erosion Response? A Review Based on Meta-Analysis of Field Rainfall Simulation Data. *J. Hydrol.* **2015**, *523*, 452–464. [[CrossRef](#)]
129. Asner, G.P.; Scurlock, J.M.O.; Hicke, J.A. Global Synthesis of Leaf Area Index Observations: Implications for Ecological and Remote Sensing Studies. *Glob. Ecol. Biogeogr.* **2003**, *12*, 191–205. [[CrossRef](#)]
130. Pereira, A.R. Adaptation of the Thornthwaite Scheme for Estimating Daily Reference Evapotranspiration. *Agric. Water Manag.* **2004**, *66*, 251–257. [[CrossRef](#)]
131. Masmoudi-Charfi, C.; Habaieb, H. Rainfall Distribution Functions for Irrigation Scheduling: Calculation Procedures Following Site of Olive (*Olea europaea* L.) Cultivation and Growing Periods. *Am. J. Plant Sci.* **2014**, *5*, 2094–2133. [[CrossRef](#)]
132. Boer, M.M.; Macfarlane, C.; Norris, J.; Sadler, R.J.; Wallace, J.; Grierson, P.F. Mapping Burned Areas and Burn Severity Patterns in SW Australian Eucalypt Forest Using Remotely-Sensed Changes in Leaf Area Index. *Remote Sens. Environ.* **2008**, *112*, 4358–4369. [[CrossRef](#)]
133. Ashby, S.F.; Falgout, R.D. A Parallel Multigrid Preconditioned Conjugate Gradient Algorithm for Groundwater Flow Simulations. *Nucl. Sci. Eng.* **1996**, *124*, 145–159. [[CrossRef](#)]
134. Maxwell, R.M. A Terrain-Following Grid Transform and Preconditioner for Parallel, Large-Scale, Integrated Hydrologic Modeling. *Adv. Water Resour.* **2013**, *53*, 109–117. [[CrossRef](#)]
135. Bréda, N.; Granier, A. Intra- and Interannual Variations of Transpiration, Leaf Area Index and Radial Growth of a Sessile Oak Stand (*Quercus petraea*). *Ann. Sci. For.* **1996**, *53*, 521–536. [[CrossRef](#)]



136. Chambers, S.D.; Beringer, J.; Randerson, J.T.; Chapin, F.S., III. Fire Effects on Net Radiation and Energy Partitioning: Contrasting Responses of Tundra and Boreal Forest Ecosystems. *J. Geophys. Res. Atmos.* **2005**, *110*. [[CrossRef](#)]
137. Allen, R.G.; Pereira, L.S.; Raes, D.; Smith, M. *Crop Evapotranspiration. Guidelines for Computing Crop Water Requirements*; FAO Irrigation and Drainage Paper; FAO: Rome, Italy, 1998.
138. Lopez-Urrea, R.; de Santa Olalla, F.M.; Fabeiro, C.; Moratalla, A. An Evaluation of Two Hourly Reference Evapotranspiration Equations for Semiarid Conditions. *Agric. Water Manag.* **2006**, *86*, 277–282. [[CrossRef](#)]
139. Allen, R.G.; Smith, M.; Perrier, A.; Pereira, L.S. An Update for the Definition of Reference Evapotranspiration. *ICID Bull.* **1994**, *43*, 1–35.
140. Niccoli, F.; Pacheco-Solana, A.; Delzon, S.; Kabala, J.P.; Asgharinia, S.; Castaldi, S.; Valentini, R.; Battipaglia, G. Effects of Wildfire on Growth, Transpiration and Hydraulic Properties of *Pinus pinaster* Aiton Forest. *Dendrochronologia* **2023**, *79*, 126086. [[CrossRef](#)]
141. Jin, Y.; Randerson, J.T.; Goetz, S.J.; Beck, P.S.A.; Loranty, M.M.; Goulden, M.L. The Influence of Burn Severity on Postfire Vegetation Recovery and Albedo Change during Early Succession in North American Boreal Forests. *J. Geophys. Res. Biogeosci.* **2012**, *117*. [[CrossRef](#)]
142. Khaleedi, J.; Lane, P.N.J.; Nitschke, C.R.; Nyman, P. Wildfire Contribution to Streamflow Variability across Australian Temperate Zone. *J. Hydrol.* **2022**, *609*, 127728. [[CrossRef](#)]
143. Cronshey, R. *Urban Hydrology for Small Watersheds*, 2nd ed.; U.S. Department of Agriculture, Soil Conservation Service, Engineering Division: Washington, DC, USA, 1986.
144. Woodward, D.E.; Hawkins, R.H.; Jiang, R.; Hjelmfelt, J.; Van Mullem, J.A.; Quan, Q.D. Runoff Curve Number Method: Examination of the Initial Abstraction Ratio. In Proceedings of the World Water & Environmental Resources Congress 2003, Philadelphia, PA, USA, 23–26 June 2003; pp. 1–10. [[CrossRef](#)]
145. Mishra, S.K.; Singh, V.P. Sediment Yield. In *Soil Conservation Service Curve Number (SCS-CN) Methodology*; Mishra, S.K., Singh, V.P., Eds.; Water Science and Technology Library; Springer Netherlands: Dordrecht, The Netherlands, 2003; pp. 436–456, ISBN 978-94-017-0147-1.
146. Kim, N.W.; Lee, J. Temporally Weighted Average Curve Number Method for Daily Runoff Simulation. *Hydrol. Process.* **2008**, *22*, 4936–4948. [[CrossRef](#)]
147. de Groen, M.M.; Savenije, H.H.G. A Monthly Interception Equation Based on the Statistical Characteristics of Daily Rainfall. *Water Resour. Res.* **2006**, *42*. [[CrossRef](#)]
148. Jarvis, P.G.; Monteith, J.L.; Weatherley, P.E. The Interpretation of the Variations in Leaf Water Potential and Stomatal Conductance Found in Canopies in the Field. *Philos. Trans. R. Soc. Lond. B Biol. Sci.* **1976**, *273*, 593–610. [[CrossRef](#)]
149. Corbari, C.; Ravazzani, G.; Galvagno, M.; Cremonese, E.; Mancini, M. Assessing Crop Coefficients for Natural Vegetated Areas Using Satellite Data and Eddy Covariance Stations. *Sensors* **2017**, *17*, 2664. [[CrossRef](#)] [[PubMed](#)]
150. Zomlot, Z.; Verbeiren, B.; Huysmans, M.; Batelaan, O. Spatial Distribution of Groundwater Recharge and Base Flow: Assessment of Controlling Factors. *J. Hydrol. Reg. Stud.* **2015**, *4*, 349–368. [[CrossRef](#)]
151. Ellison, D. Trees, Forests and Water: Cool Insights for a Hot World. *Glob. Environ. Chang.* **2017**, *43*, 51–61. [[CrossRef](#)]
152. Ilstedt, U. Intermediate Tree Cover Can Maximize Groundwater Recharge in the Seasonally Dry Tropics. *Sci. Rep.* **2016**, *6*, 21930. [[CrossRef](#)]
153. de Oliveira, J.V.; Ferreira, D.B.; Sahoo, P.K.; Sodré, G.R.C.; de Souza, E.B.; Queiroz, J.C.B. Differences in Precipitation and Evapotranspiration between Forested and Deforested Areas in the Amazon Rainforest Using Remote Sensing Data. *Environ. Earth Sci.* **2018**, *77*, 239. [[CrossRef](#)]
154. Byram, G.M.; Jemison, G.M. Solar Radiation and Forest Fuel Moisture. *J. Agric. Res.* **1943**, *67*, 149.
155. Belcher, S.E.; Harman, I.N.; Finnigan, J.J. The Wind in the Willows: Flows in Forest Canopies in Complex Terrain. *Annu. Rev. Fluid Mech.* **2012**, *44*, 479–504. [[CrossRef](#)]
156. Montes-Helu, M.C.; Montes-Helu, M.C. Persistent Effects of Fire-Induced Vegetation Change on Energy Partitioning and Evapotranspiration in Ponderosa Pine Forests. *Agric. For. Meteorol.* **2009**, *149*, 491–500. [[CrossRef](#)]
157. Suggitt, A.J. Habitat Microclimates Drive Fine-scale Variation in Extreme Temperatures. *Oikos* **2011**, *120*, 1–8. [[CrossRef](#)]
158. von Arx, G.; Graf Pannatier, E.; Thimonier, A.; Rebetez, M. Microclimate in Forests with Varying Leaf Area Index and Soil Moisture: Potential Implications for Seedling Establishment in a Changing Climate. *J. Ecol.* **2013**, *101*, 1201–1213. [[CrossRef](#)]
159. De Frenne, P.; Zellweger, F.; Rodríguez-Sánchez, F.; Scheffers, B.R.; Hylander, K.; Luoto, M.; Vellend, M.; Verheyen, K.; Lenoir, J. Global Buffering of Temperatures under Forest Canopies. *Nat. Ecol. Evol.* **2019**, *3*, 744–749. [[CrossRef](#)] [[PubMed](#)]
160. Davis, K.T. Microclimatic Buffering in Forests of the Future: The Role of Local Water Balance. *Ecography* **2019**, *42*, 1–11. [[CrossRef](#)]
161. Wolf, K.D. Wildfire Impacts on Forest Microclimate Vary with Biophysical Context. *Ecosphere* **2021**, *12*, e03467. [[CrossRef](#)]
162. Ripley, E.A.; Archibold, O.W. Effects of Burning on Prairie Aspen Grove Microclimate. *Agric. Ecosyst. Environ.* **1999**, *72*, 227–237. [[CrossRef](#)]
163. Liu, Z.; Ballantyne, A.P.; Cooper, L.A. Biophysical Feedback of Global Forest Fires on Surface Temperature. *Nat. Commun.* **2019**, *10*, 214. [[CrossRef](#)]
164. Arcenegui, V.; Guerrero, C.; Mataix-Solera, J.; Mataix-Beneyto, J.; Zornoza, R.; Morales, J.; Mayoral, A.M. The Presence of Ash as an Interference Factor in the Estimation of the Maximum Temperature Reached in Burned Soils Using Near-Infrared Spectroscopy (NIR). *Catena* **2008**, *74*, 177–184. [[CrossRef](#)]

165. Chiodi, A.M.; Potter, B.E.; Larkin, N.K. Multi-Decadal Change in Western US Nighttime Vapor Pressure Deficit. *Geophys. Res. Lett.* **2021**, *48*, e2021GL092830. [[CrossRef](#)]
166. Jódar, J.; Carpintero, E.; Martos-Rosillo, S.; Ruiz-Constán, A.; Marín-Lechado, C.; Cabrera-Arrabal, J.A.; Navarrete-Mazariegos, E.; González-Ramón, A.; Lambán, L.J.; Herrera, C.; et al. Combination of Lumped Hydrological and Remote-Sensing Models to Evaluate Water Resources in a Semi-Arid High Altitude Ungauged Watershed of Sierra Nevada (Southern Spain). *Sci. Total Environ.* **2018**, *625*, 285–300. [[CrossRef](#)]
167. Scanlon, B.R.; Longuevergne, L.; Long, D. Ground Referencing GRACE Satellite Estimates of Groundwater Storage Changes in the California Central Valley, USA. *Water Resour. Res.* **2012**, *48*. [[CrossRef](#)]
168. Jiang, D.; Wang, J.; Huang, Y.; Zhou, K.; Ding, X.; Fu, J. The Review of GRACE Data Applications in Terrestrial Hydrology Monitoring. *Adv. Meteorol.* **2014**, *2014*, 725131. [[CrossRef](#)]
169. Frappart, F.; Ramillien, G. Monitoring Groundwater Storage Changes Using the Gravity Recovery and Climate Experiment (GRACE) Satellite Mission: A Review. *Remote Sens.* **2018**, *10*, 829. [[CrossRef](#)]
170. He, L.; Valocchi, A.J.; Duarte, C.A. An Adaptive Global–Local Generalized FEM for Multiscale Advection–Diffusion Problems. *Comput. Methods Appl. Mech. Eng.* **2024**, *418*, 116548. [[CrossRef](#)]
171. Davis Todd, C.E.; Goss, A.M.; Tripathy, D.; Harbor, J.M. The Effects of Landscape Transformation in a Changing Climate on Local Water Resources. *Phys. Geogr.* **2007**, *28*, 21–36. [[CrossRef](#)]
172. Akay, H.; Baduna Koçyiğit, M.; Yanmaz, A.M. Effect of Using Multiple Stream Gauging Stations on Calibration of Hydrologic Parameters and Estimation of Hydrograph of Ungauged Neighboring Basin. *Arab. J. Geosci.* **2018**, *11*, 282. [[CrossRef](#)]

**Disclaimer/Publisher’s Note:** The statements, opinions and data contained in all publications are solely those of the individual author(s) and contributor(s) and not of MDPI and/or the editor(s). MDPI and/or the editor(s) disclaim responsibility for any injury to people or property resulting from any ideas, methods, instructions or products referred to in the content.